AD-A118 384 SOUTHWEST RESEARCH INST SAN ANTONIO TX F/G 13/6
ANALYSIS AND EXPERIMENTAL VERIFICATION OF A COMBUSTING PROPANE --ETC(U)
AUG 82 J L RAND, J F POLK DAAK11-77-C-0085
UNCLASSIFIED SWRI-02-5045-002 ARBRL-CR-00486 NL

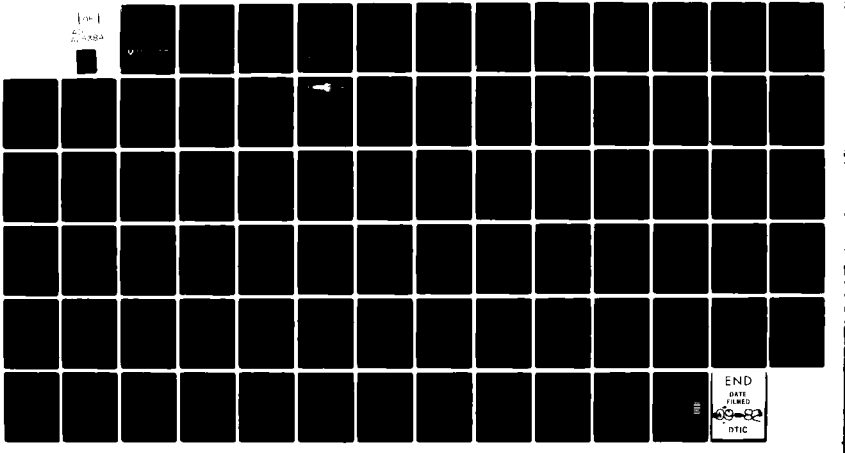

12

CONTRACT REPORT ARBRL-CR-00486

ANALYSIS AND EXPERIMENTAL VERIFICATION OF A COMBUSTING PROPANE TORCH MODEL

Prepared by

Southwest Research Institute
6220 Culebra Road
San Antonio, TX 78284

August 1982

US ARMY ARMAMENT RESEARCH AND DEVELOPMENT COMMAND
BALLISTIC RESEARCH LABORATORY
ABERDEEN PROVING GROUND, MARYLAND

Destroy this report when it is no longer needed.
Do not return it to the originator.

Secondary distribution of this report is prohibited.

Additional copies of this report may be obtained from the National Technical Information Service, U. S. Department of Commerce, Springfield, Virginia 22161.

The findings in this report are not to be construed as an official Department of the Army position, unless so designated by other authorized documents.

The use of trade names or manufacturers' names in this report does not constitute indorsement of any commercial product.

SECURITY CLASSIFICATION OF THIS PAGE (When Data Entered)

REPORT DOCUMENTATION PAGE		READ INSTRUCTIONS BEFORE COMPLETING FORM
1. REPORT NUMBER Contract Report ARBRL-CR-00486	2. GOVT ACCESSION NO. AD-A118 384	3. RECIPIENT'S CATALOG NUMBER
4. TITLE (and Subtitle) Analysis and Experimental Verification of a Combusting Propane Torch Model		5. TYPE OF REPORT & PERIOD COVERED Final
		6. PERFORMING ORG. REPORT NUMBER 02-5045-002
7. AUTHOR(s) James L. Rand and John F. Polk		8. CONTRACT OR GRANT NUMBER(s) DAAK11-77-C-0085
9. PERFORMING ORGANIZATION NAME AND ADDRESS Southwest Research Institute 6220 Culebra Road, P.O. Drawer 28510 San Antonio, TX 78284		10. PROGRAM ELEMENT, PROJECT, TASK AREA & WORK UNIT NUMBERS
11. CONTROLLING OFFICE NAME AND ADDRESS US Army Armament Research and Development Command US Army Ballistic Research Laboratory (DRDAR-BL) Aberdeen Proving Ground, MD 21005		12. REPORT DATE August 1982 13. NUMBER OF PAGES 84
14. MONITORING AGENCY NAME & ADDRESS(if different from Controlling Office)		15. SECURITY CLASS. (of this report) Unclassified 15a. DECLASSIFICATION/DOWNGRADING SCHEDULE

16. DISTRIBUTION STATEMENT (of this Report)

Approved for public release; distribution unlimited.

17. DISTRIBUTION STATEMENT (of the abstract entered in Block 20, if different from Report)

18. SUPPLEMENTARY NOTES

19. KEY WORDS (Continue on reverse side if necessary and identify by block number)

Propane, LPG, Torching, Two-Phase Flow, Tank Car, Rail Safety

20. ABSTRACT (Continue on reverse side if necessary and identify by block number)

A model for turbulent mixing with air of a two-phase propane combusting jet and subsequent inpingement on a downstream target plate is used to predict the results obtained from the BRL/DOT Torch Simulation Facility. Experimental data is in excellent agreement with predicted characteristics such as velocity and heat flux. Combustion occurs with fuel lean mixtures where the ratio of air to propane mass varies from stoichiometric to 21 percent above stoichiometric.

DD FORM 1 JAN 73 1473 EDITION OF 1 NOV 65 IS OBSOLETE

UNCLASSIFIED

SECURITY CLASSIFICATION OF THIS PAGE (When Data Entered)

ACKNOWLEDGMENTS

The author is grateful to Dr. Charles E. Anderson, Jr., for his helpful comments, suggestions and cooperation during the course of this investigation. Also, the author wishes to acknowledge the following SwRI staff members for their contribution to this program.

Dr. Franklin T. Dodge and Mr. William J. Astleford for their initial efforts and continuing support in the development of the real gas effects in the fuel.

Mr. Mark G. Whitney and Ms. Patricia K Moseley for their assistance in the programming and numerical evaluation of the various models.

The cooperation of these individuals and others is greatly appreciated.

STATEMENT OF ATTRIBUTION

The present document is a composite of two reports entitled "An Analytical Model of a Two Phase Propane Combusting Jet" and "Experimental Verification of a Combusting LPG Torch Model", which are prepared by James L. Rand of Southwest Research Institute, under contract DAAK11-77-C-0085. After internal review at BRL it was decided that a single report would suffice. The previous reports were therefore edited and combined into the present form by Dr. John F. Polk of the Target Effects Branch, BRL.

TABLE OF CONTENTS

LIST OF ILLUSTRATIONS

LIST OF TABLES

LIST OF SYMBOLS

Symbol	Meaning	Page
A	cross section area	17
C_D	discharge coefficient	17
C_p	coef. of specific heat at constant pressure	17
h	enthalpy	17
h	heat transfer coefficient	34
k	empirical viscosity coefficient	25
m	mass ratio (air to fuel)	20
$\dot{m}$	mass flow rate	17
M_o	jet Mach number	25
MW	molecular weight	24
Nu	Nusselt number	34
Pr	Prandtl number	34
$\dot{q}$	heat flux	35
r	radial coordinate	30
$r_{.5}$	radial coordinate for half-velocity	30
R	stagnation radius	34
Re	Reynolds number	34
S	entropy	17
T	temperature	36
U	flow velocity	17
v	specific volume	17
X	mixture ratio	16
$\bar{X}$	non-dimensional axial coordinate	25
Z	distance from wall	31

LIST OF SYMBOLS (CONTINUED)

Symbol	Meaning	Page
α , β	empirical constants	36
γ	ratio of specific heats	24
ϵ	emissivity	36
ν	kinematic viscosity	34
ρ	fluid density	17
σ	Stefan-Boltzmann constant	36
	SUBSCRIPTS	
o	axial station where combustion is complete	22
1	axial station where mixing is complete	20
e	orifice exit station	18
C	centerline	30
F	flame	36
FR	fluid, reservoir conditions	17
GR	gas, reservoir conditions	17
P	plate	36
R	reservoir condition	17
R	stagnation coordinate	34

I. INTRODUCTION

A rash of railway accidents involving tank cars carrying flammable materials such as propane and vinyl chloride prompted an investigation by the Federal Railroad Administration (FRA) of the Department of Transportation. Because of the Ballistic Research Laboratory's (BRL) knowledge in fire technology and skills in high-temperature measurements, the FRA sought out the BRL for assistance. A series of field experiments on one-fifth-scale model tank cars culminated in two full-scale pool fire tests on rail tank cars filled with propane.

For the first test, a bare car was placed in a pit, instrumented and filled with approximately 113.5 kl (30,000 gallons) of propane. The car was then completely engulfed in flames (JP-4 jet fuel was used to provide the source of the fire). After 24.5 minutes of fire exposure, the tank violently ruptured, spewing fire and debris considerable distances. Armed with the data from the test, post-test analyses of the fragments, metallurgical analyses, etc., the mechanism of failure was understood and documented.[1]

Propane and vinyl chloride are shipped under pressure in the liquid form. In a fire environment, heat is transferred to the interior of the car. The temperature of the contents is raised and the pressure increases. Above a specified pressure, the relief valve opens and vents, but the pressure will continue to climb if the total heat to the interior is great enough. In addition, the steel tank shell is heated, particularly that portion which is not in contact with the liquid. As the metal heats, its strength begins to degrade, especially where metal temperatures are in excess of 425°C (800°F). If exposed to the fire long enough, stresses induced by the interior pressure exceed the strength of the temperature-weakened steel. A sudden release of the pressurized contents then occurs, vaporizes, mixes with air, and an explosion occurs. This fuel/air explosion can "rocket" portions of a tank car for considerable distance, create a tremendous fireball and a damaging blast wave.

The second full-scale test was on an insulated car, and it was demonstrated that by protecting the metal skin from reaching elevated temperatures, the car would retain its integrity while releasing its contents through the relief valve until the car was essentially empty. Also, the rupture, if indeed it did rupture, would be significantly less violent.[2]

---

[1] *Charles Anderson, William Townsend, John A. Zook, Gregory Cowgill, "The Effects of a Fire Environment on a Rail Tank Car Filled With LPG," BRL R 1935, USA Ballistic Research Laboratories, Aberdeen Proving Ground, MD, September 1976. (AD B015605L)*

[2] *Charles Anderson, William Townsend, John Zook, Gregory Cowgill, "The Comparison of Thermally Coated and Uninsulated Rail Tank Cars Filled With LPG Subjected to a Fire Environment," Report No. FRA-OR8 D 75-32, National Technical Information Service, Springfield, VA, December 1974.*

However, accident investigations showed that a significant percentage of ruptures, where there were reliable estimates for the times, occurred in less than 24.5 minutes. Yet, full-scale testing of the base car was a full engulfment pool fire - a "worst case" test. Hence, another mechanism was identified as contributing to tank car failures - the "torch" mechanism.

A torch can result from ignited liquid and/or vapor rushing out of a hole or tear in the shell. This could be caused by a coupler impact in an accident, or possible effluent from a relief valve on an overturned car impinging on an adjacent car. Remembering that the contents are already under pressure, and that any additional heat from a fire would raise the internal pressure, the ignited, high velocity stream acts as as large blowtorch. High heat fluxes from the torch can heat the impinged steel to dangerously high temperatures in only several minutes.

To investigate this phenomenon, the BRL designed, constructed, and operates a torch simulator facility at the DOT Transportation Test Center, Pueblo, Colorado.[3] There, the BRL tests the thermal response of steel plates with various types of thermal insulating systems for possible applications to rail tank cars.[4] The torch is formed by the blowdown of pressurized propane vapor and liquid from a 1.9 kl (500 gallon) tank, Figure 1. The vapor and liquid are combined in a manifold prior to expansion through a 0.95 cm (3/8-in) orifice. The resulting high-velocity jet is initially ignited and the resulting torch (a turbulent diffusion flame) impinges on the test plate.

Analyses of the torch velocity, its downstream lateral spreading, and the heat flux to the plate are useful for several reasons. Initially, BRL needed guidelines to help design the tests. Then, after demonstrating that a torch-like test is a reliable way to characterize the performance of thermal coatings, BRL wanted to understand the effects of various parameters and learn what scaling parameters characterize the torch. For small-scale tests, an analysis is needed to specify the torch parameters that adequately simulate large-scale heat fluxes. Southwest Research Institute, therefore, was requested by BRL to analyze the fluid dynamics and thermodynamics of a high-speed propane torch impinging upon a plate, to include propane jet formation and combustion.

---

[3] *William Townsend and Richard Markland, "Preparation of the BRL Tank Car Torch Facility at the DOT Transportation Test Center, Pueblo, Colorado," BRL unpublished report, USA Ballistic Research Laboratories, Aberdeen Proving Ground, MD, September 1975.*

[4] *Charles Anderson, William Townsend, Richard Markland, John Zook, "Comparison of Various Thermal Systems for the Protection of Rail Tank Cars Tested at the FRA/BRL Torching Facility," BRL unpublished report, USA Ballistic Research Laboratories, Aberdeen Proving Ground, MD, December 1975.*

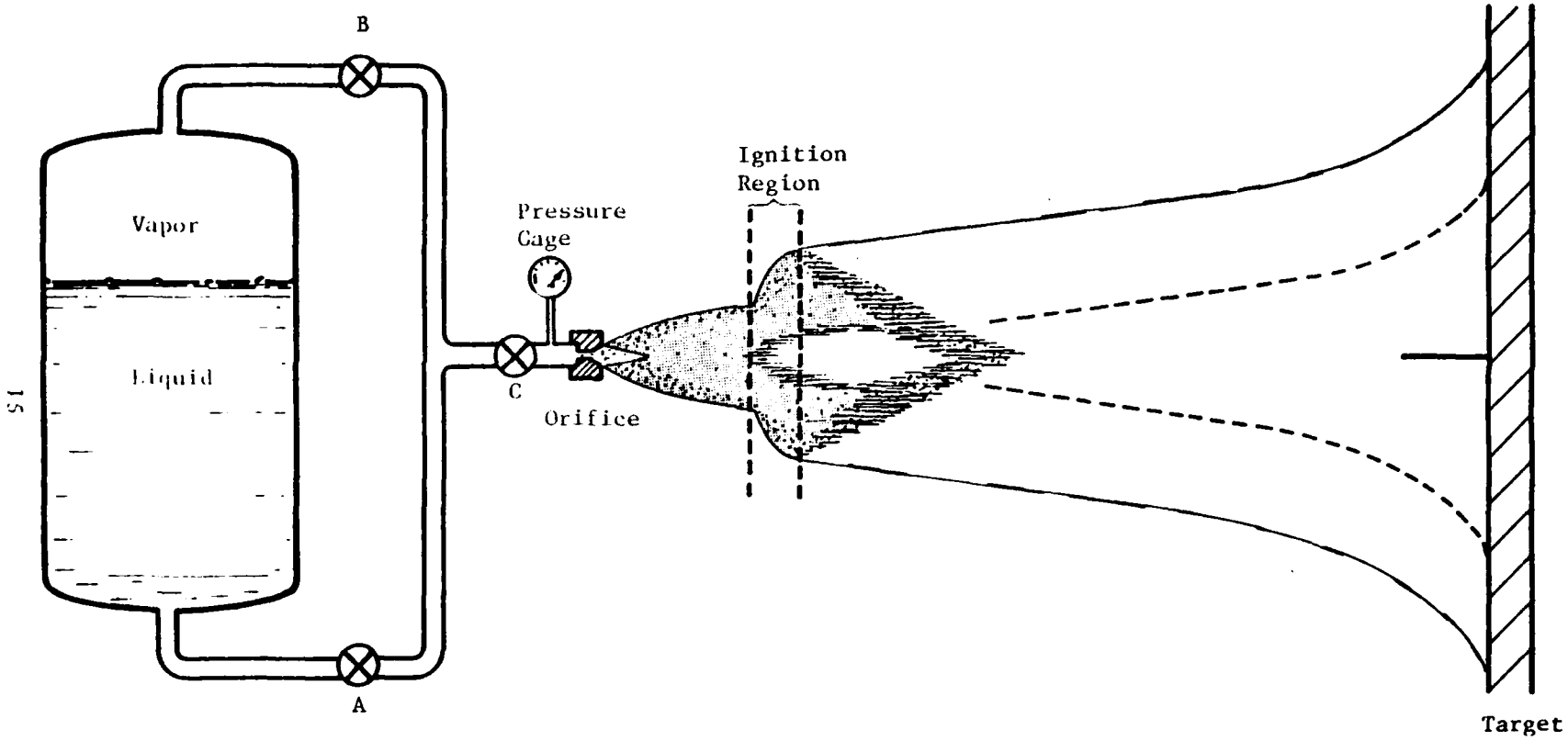

Figure 1. Schematic Representation of Two-Phase Torch Test

II. JET ANALYSIS[5]

At the exit plane of the propane tank orifice, a two-phase propane jet emerges at supersonic velocities as the high pressure fuel expands to atmospheric pressure. The jet then spreads laterally by the turbulent entrainment of air. Ignition can occur where sufficient air has been entrained to support combustion. At this point, a new jet is formed by the products of combustion and continues to spread laterally as more air is entrained through the turbulent mixing process. As the jet nears the target plate, the flow is turned, which causes a decrease in the centerline velocity of the jet, and a wall jet is formed.

A rigorous two-dimensional treatment of this problem may be possible by using techniques such as those reported by Spalding.[6] However, for speed and efficiency, a simple analysis has been developed by combining a number of one-dimensional solutions available in the literature. This approach is relatively straightforward, physically sound and sufficiently accurate to explain observed experimental phenomena.

A. Reservoir Expansion

The propane torch analysis is initiated by establishing the state of the fuel upstream of the orifice. Referring to Figure 1, it is assumed that a mixture of saturated vapor and saturated liquid occurs in the manifold upstream of the orifice. The pressure is monitored at this point during the test; however, this is insufficient to establish the thermodynamic state of the mixture. Since the propane is a mixture of both vapor and liquid, the relative amounts of these two phases must be established in order to determine the thermodynamic state of the reservoir. This is accomplished by defining the "quality" of the mixture as the ratio of the mass of vapor to the total mass of the mixture. A quality of one represents a pure vapor flow, while a quality of zero represents a pure liquid flow. It is possible to control the quality of the mixture by a suitable adjustment of valves A and B shown in Figure 1. For the purpose of this analysis, the reservoir quality, XR, will be assumed to be known.

The thermodynamic properties of propane are known and have been inserted into this analysis in tabular form. The reservoir temperature is found by linear interpolation of the reservoir pressure since the temperature is independent of quality. The remaining state variables, such as entropy, enthalpy and specific volume, are then found on the basis of the assumed quality.

---

[5] *A more complete description of the modeling is given in "An Analytical Model of a Two-Phase Propane Combusting Jet," James L. Rand, Report 02-5045-001, Southwest Research Institute, San Antonio, TX, November 1980.*

[6] *Spalding, D.B., "A Simple Model on the Rate of Turbulent Combustion," Turbulent Combustion, Progress in Astronautics and Aeronautics, Vol. 58, AIAA, 1978, pp. 105-116.*

$$S_R = (1 - X)\, S_{FR} + (X)\, S_{GR} \tag{1.a}$$

$$h_R = (1 - X)\, h_{FR} + (X)\, h_{GR} \tag{1.b}$$

$$v_R = (1 - X)\, v_{FR} + (X)\, v_{GR} \tag{1.c}$$

The thermodynamic properties on the right-hand side of these equations are determined from the tabular data in the same manner as the temperature.

After determining the reservoir conditions, the fuel is then expanded from the measured high pressure through a 0.95-cm orifice to ambient pressure. In a previous report[7] the fuel was considered to be an ideal gas which permitted the jet throat and exit velocities as well as state variables to be determined analytically. However, due to the saturated nature of the reservoir, a numerical technique was developed which would permit the expansion of the propane along an isentrope through the orifice to the final jet exit conditions.

The procedure used to obtain the expanded fuel conditions is based on holding the entropy determined in equation 1 invariant as the pressure is reduced. If the flow is assumed to be choked at the orifice, then conditions at the throat will result in the maximum flow rate. Since the effective area of the orifice is relatively insensitive to small changes in pressure, the maximum flow rate will coincide with the conditions for maximum mass flux, $\rho_T U_T$. The density at the throat, ρ_T, is found by incrementally reducing the pressure and computing the quality required to maintain the same entropy. Having determined the quality, the enthalpy, h_T, may be evaluated and the flow velocity computed from the energy equation:

$$h_T + \frac{1}{2} U_T^2 = h_R \tag{2}$$

This process is repeated until the pressure for a maximum value for the mass flux is found. Once this is determined all other thermodynamic properties may be found at the throat. The mass flow is determined from the product of the effective area of the throat and the mass flux.

$$\dot{m} = \rho_T U_T A_T C_D \tag{3}$$

The coefficient, C_D, may be considered to be a discharge coefficient which accounts for the vena contracta at the orifice. The value of this coefficient may be adjusted on the basis of experimental observations; however, for a ratio of orifice diameter to inlet pipe diameter less than 0.2, a value of 0.5 appears to be applicable over a large range of Reynolds numbers.

---

[7] *Astleford, W.J. and Dodge, F.T., "Response of Fuel Targets to Munitions: Heat Transfer Analysis of Torches Impinging on Plates," SWRI Report NO. 02-3669, June 1977.*

The exit conditions from the orifice may be found by further expansion of the propane to ambient pressure. If the exit conditions are assumed to be one atmosphere, then the fuel will exit at a temperature of 231°K. The quality of the flow may be found from equation 1 where the values of S_{FR} and S_{GR} are known from the table of thermodynamic properties at one atmosphere. Once the exit quality is established, all other static properties of the flow may be computed. As before, the velocity is computed from the change in enthalpy of the flow from the reservoir enthalpy. Typical results which show the influence of reservoir conditions on the exit velocity are shown in Figure 2.

The exit area is computed on the basis of the mass flow rate previously computed at the throat of the nozzle.

$$A_e = \frac{\rho_T U_T A_T C_D}{\rho_e U_e} \tag{4}$$

At this point, all flow conditions are known for the fuel as it is injected into ambient air considered to be at rest.

B. Mixing Model

A wealth of literature exists on the expansion and turbulent mixing of a free jet. The work of Kleinstein[8] and Witze[9] show remarkably good agreement with nonreacting jet mixing experiments. Portions of their work were used in a prior report[7] on this subject. However, in order to simplify the analysis here and maintain the one dimensionality of this technique, a simplified mixing theory has been developed for this program.

It is observed that as the fuel exits the nozzle no air has yet been mixed with the fuel so that combustion cannot occur. The flammability limits in air of propane are from 2.1% to 10.1% by volume. Therefore, as the fuel jet expands, the mixture will reach a rich flammable condition first and then approach the stoichiometric ratio further downstream. In addition, the flow velocity of the fuel-air mixture must be slow enough to sustain combustion. In the following analysis, the fuel and air will be assumed to be thoroughly mixed, which is a departure from those assumptions contained in References 8 and 9, but should be sufficient to allow an estimate of the products of combustion.

It is realized that there exists conditions in which there is an unburned core of fuel-rich propane, with burning on the periphery. As the initial conditions go to more and more liquid (i.e., the quality goes toward zero), it is expected that this fuel-rich core condition will become more prevalent (and indeed, this is what is observed). The modeling assumption is, therefore, not as well met as when the quality is closer to one.

---

[8] *Kleinstein, G., "Mixing in Turbulent Axially Symmetric Free Jets," J. Spacecraft & Rockets, 1, July-August 964. pp.403-408.*

[9] *Witze, P., "Centerline Velocity Decay of Compressible Free Jet," J. Spacecraft & Rockets, 12, April 1974, pp 417-418.*

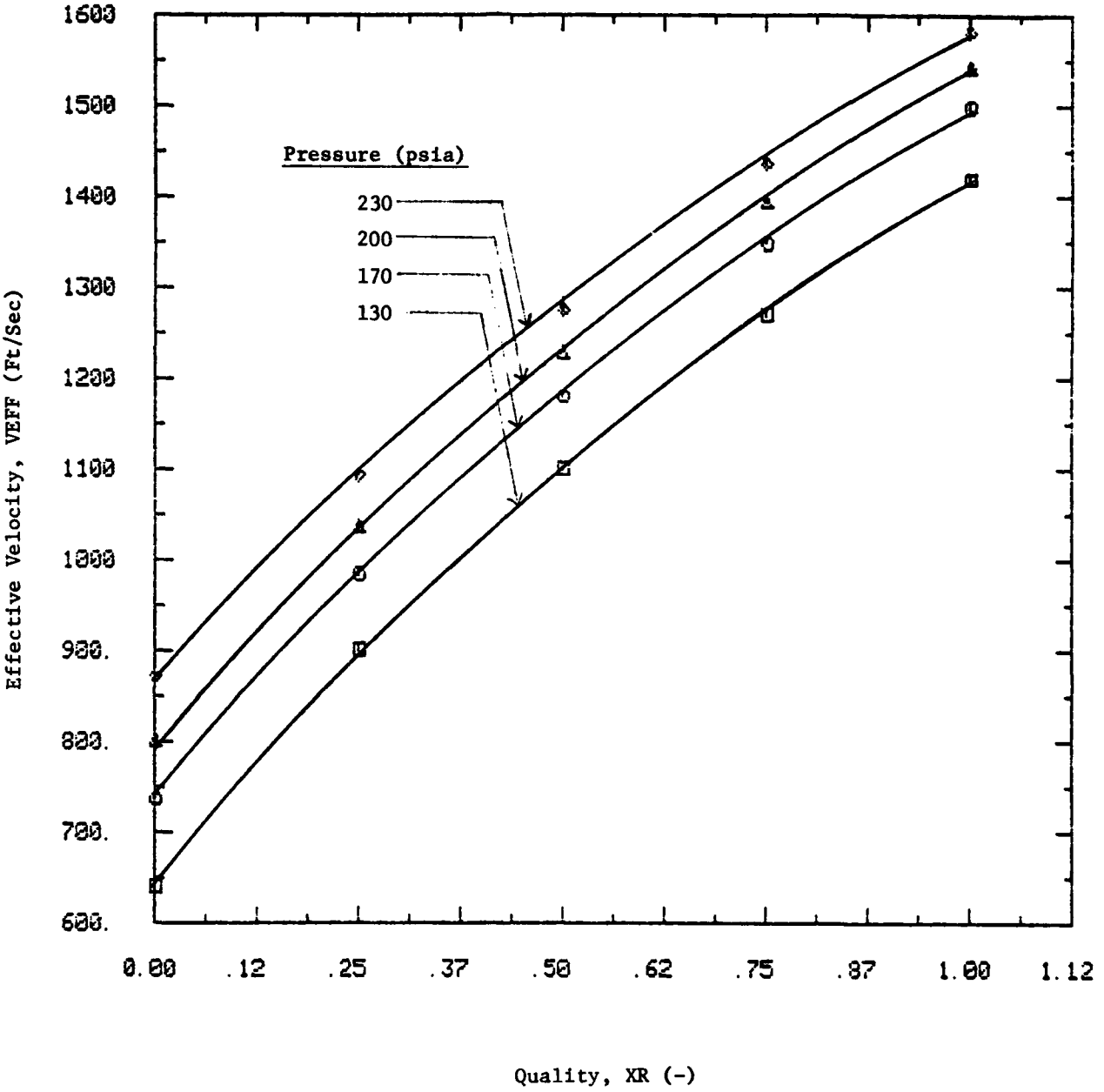

Figure 2. Effect of Reservoir Conditions on Exit Velocity

In order to determine the relationship between the velocities and mass ratios, an analytic model has been developed on the basis of the conservation of mass and momentum assuming the torch does not change with time. The steady flow situation is depicted in Figure 3(a). Two regions of interest will be considered separately. The first region from the orifice exit to point 1 is a region where mixing occurs without combustion. The second region, from point 1 to point 0, is where instantaneous combustion will be assumed to occur without the addition of air. The conditions at point 0 will be assumed to be the starting conditions for turbulent mixing of a free jet formed by the combustion products.

A control volume is drawn around the region from the orifice exit to point 1 as shown in Figure 3(b). The sides of this control volume are parallel to the centerline and sufficiently far away that the velocity of the air crossing this boundary is small. It should be noted that the velocity of the pure propane fuel crossing the left-hand boundary is supersonic. Applying the principal of conservation of mass, for this assumed steady flow, the mass flow rate of the mixture is given by:

$$\rho_e A_e U_e + (\rho AU)_{air} = \rho_1 A_1 U_1$$

If the flow is steady, then the ratio of the mass of air to the mass of fuel must be the same as the ratio of the mass rates of flow. Therefore, the mass ratio will be defined as:

$$m \equiv \frac{(\rho AU)_{air}}{\rho_e A_e U_e}$$

Thus the previous equation may now be written in terms of the known mass flow rate of fuel and the mass ratio as:

$$\rho_1 A_1 U_1 = (1 + m)\ \rho_e A_e U_e \qquad (5)$$

Applying the principle of conservation of momentum in the axial direction:

$$(pA)_e + \left(\rho_e A_e U_e\right) U_e + (\rho AU)_{air}\, U_{air} = (pA)_1 + \left(\rho_1 A_1 U_1\right) U_1$$

Since the pressure at all points on the boundary of this control volume is equal to the ambient pressure, the external force terms are self equilibrating. The axial component of the air crossing the lateral boundaries is assumed to be zero by the judicious location of the boundary. Therefore, this equation may be reduced to the following:

$$U_1 = \left(\frac{\rho_e A_e U_e}{\rho_1 A_1 U_1}\right) U_e$$

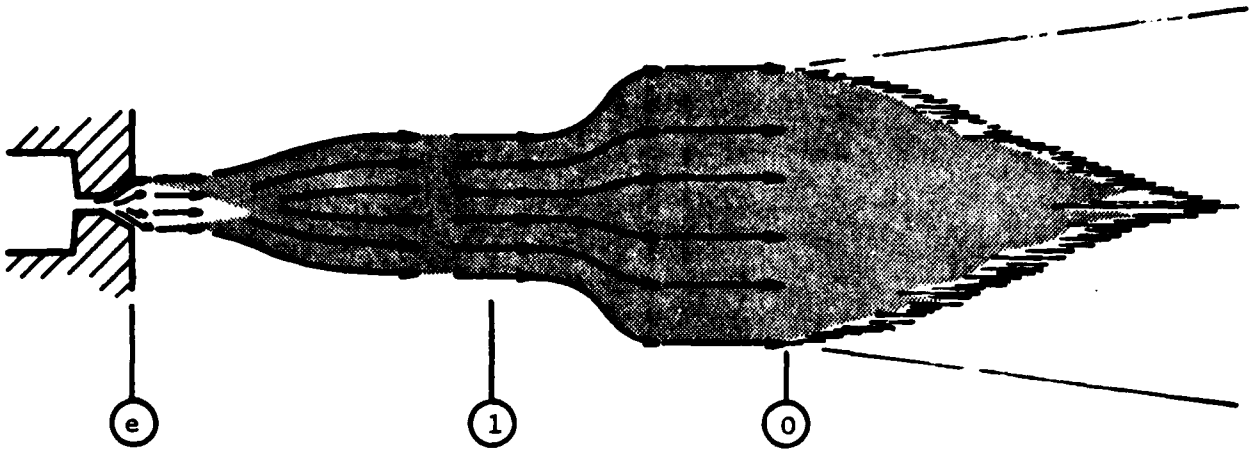

(a) Model of Jet Starting Condition

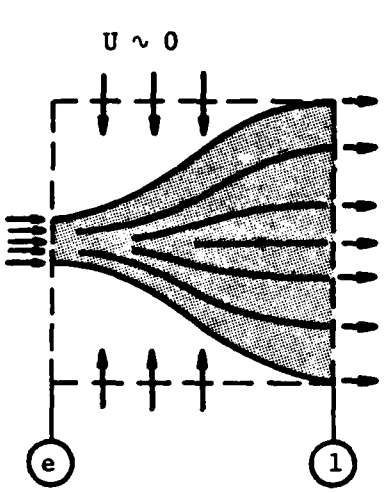

(b) Initial Mixing Region

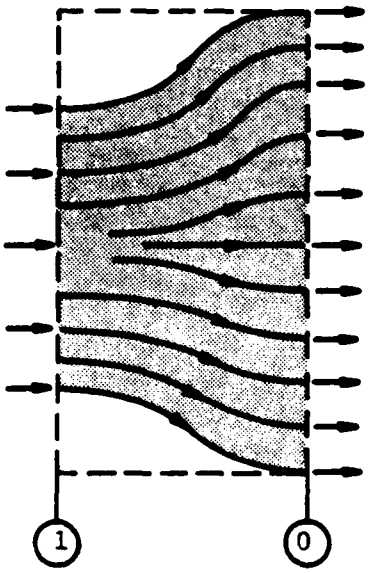

(c) Combustion Region

Figure 3. Schematic of Jet Starting Conditions

Incorporating equation 5 into the resulting momentum equation yields the velocity of the mixture in terms of the mass ratio and the propane exit velocity.

$$U_1 = \frac{U_e}{(1 + m)}$$

Applying the same reasoning to the combustion region shown in Figure 3(c), conservation of mass yields:

$$\rho_o A_o U_o = \rho_1 A_1 U_1 = (1 + m)\ \rho_e A_e U_e$$

Combining this with conservation of momentum:

$$U_o = U_1 = \frac{U_e}{(1 + m)} \tag{6}$$

The area over which the combustion products are moving at a velocity of U_o, is determined from the mass flow rate. Therefore,

$$A_o = (1 + m)^2 \left(\frac{\rho_e}{\rho_o}\right) A_e \tag{7}$$

In order to compute this area, it is first necessary to evaluate the density of the combustion products. It should be noted that the energy equation has not yet been used.

C. Combustion Process

In order to determine the thermodynamic properties of the combustion products for a given ratio of oxidizer to fuel, a program developed by NASA Lewis Research Center[10] was found to be very useful. The combustion of propane and air is a complex chemical equilibrium process which results in the conversion of energy into a sensible form, the creation of new species and the destruction of others. The program, CEC76, is the latest version and is capable of computing the theoretical thermodynamic properties of products of combustion at constant pressure and energy.

---

[10] *Gordon, S. and McBride, B.J., "Computer Program for Calculation of Complex Chemical Equilibrium Composition, Rocket Performance, Incident and Reflected Shocks, and Chapman-Jouguet Detonations," NASA Lewis Research Center NASA SP-273, March 1976.*

The program is based on the minimization of the Gibbs free energy rather than the use of equilibrium constants and is assumed to be a static process.

In order to relate the results of the combustion computations to the present problem, a method was developed to account for the various parameters which may change in the torch test. The propane fuel, originally at high pressure, will be injected into air at a temperature corresponding to saturated propane vapor at one atmosphere. This temperature is 231°C unless the flow is superheated by some nonisentropic process prior to injection. The air is assumed to be at rest with a pressure and temperature of one atmosphere and 298°K, respectively. The variables which may influence the thermodynamic properties of the products of combustion include the quality of the expanded propane jet and the energy of the flow which may be represented by the total enthalpy of the jet. In addition to these variables, the mass ratio of air to propane, m, plays a significant role in the efficiency of combustion, the formation of species and the resulting flame temperature as well as other thermodynamic properties.

The NASA program, CEC76, is very general and far more inclusive than that needed for this particular problem. Therefore, a data base was generated with the program and the results modeled for use in the TORCH program. The most sensitive thermodynamic property for this problem is the flame temperature. It is assumed that this temperature can be expressed explicitly as a function of quality and velocity and implicitly as a function of mass ratio. The velocity as used here is a measure of the total enthalpy of the propane jet. The flame temperature may then be expressed as:

$$T = T\ (X,\ U;\ m)$$

A Taylor series expansion

$$T\ (X,\ U;\ m) = T\ (0,\ 0;\ m) + \left(\frac{\partial T}{\partial X}\right)_{U=0} X + \left(\frac{\partial T}{\partial U}\right)_{X=0} U \qquad (8)$$

stipulates that the flame temperature for any quality or velocity may be found from the temperature and its derivatives evaluated at a quality of zero, pure liquid, and zero velocity. The reference temperature and its derivatives in this case remain a function of mass ratio. The combustion program was exercised with a variety of mass ratios, qualities, and velocities. It was found that for any given mass ratio, the change in temperature for any given change in quality or velocity was linear, indicating that the first order Taylor series to be a good approximation.

Likewise, the enthalpy can be written as:

$$h\ (X,m\ ) = h\ (0;\ m) + \left(\frac{\partial h}{\partial X}\right) X \qquad (9)$$

Molecular weight, MW, and specific heat ratio, γ, were found to depend on the mass ratio but to be virtually independent of quality. The remaining properties such as density and sound speed can be computed assuming the ideal gas law since even pure propane vapor at atmospheric pressure and temperature will behave in this manner.

The functional dependence of temperature, enthalpy, molecular weight, and specific heat on mass ratio were computed for mass ratios less than stoichiometric (m = 17.3) and also for fuel lean mixtures. It was found that simple polynomial expressions could be used for the entire range of mass ratios with the exception of the ratio of specific heats, which had to be fitted in two regions. The results are given in Table 1.

Table 1. Polynomial Coefficients, a_n

$$F\ (0,\ 0\ ;\ m) = \sum_{n\ =\ 0}^{4} a_n\ m^n$$

n	T (0, 0; m)	MW (m) (g/mole)	γ (m) (m < 17.3)	γ (m) (m > 17.3)	h (0; m) (cal/g)
0	-9.3681 E+2	1.283 E+1	1.3635	1.3296 E-1	-1.939 E+2
1	4.3158 E+2	1.8229 E+0	-8.254 E-3	1.2014 E-1	2.2579 E+1
2	-1.9206 E+1	-6.9251 E-2	0	-4.2735 E-3	-1.2611 E+0
3	2.5115 E-1	8.6095 E-4	0	5.1369 E-5	3.3207 E-2
4	0	0	0	0	3.303 E-4

The functional form of the partial derivations in Equations (8) and (9) were found to be:

$$\left(\frac{\partial T}{\partial X}\right)_{U=0} = -2.4734\ m + 50.73\ (^{\circ}K) \qquad (10)$$

$$\left(\frac{\partial T}{\partial U}\right)_{X=0} = (-1.41\ m + 28.894) \times 10^{-5}\ (°k\ sec/cm) \qquad (11)$$

$$\left(\frac{\partial h}{\partial X}\right) = 0.182\ h\ (0;\ m)\ (cal/g) \qquad (12)$$

The coefficients of the various terms were determined by minimizing the square of the deviation of the assumed equation from the numerical results of the combustion program. A comparison between the thermodynamic quantities computed by the NASA program and the fitted polynomials is shown in Figures 4-7.

D. Turbulent Mixing

The mass ratio, m, is obviously an important parameter. The amount of air entrained is a function of downstream position and jet velocity. Analysis of the centerline velocity decay and lateral spreading of the jet follows the basic theory of Schlichting[11] as modified by more recent work.

The centerline velocity, U_c, of the jet is reduced by the entrainment of air due to turbulent mixing. The decay may be expressed quantitatively as:

$$U_c\ (\bar{X}) = U_0 \left\{ 1 - \exp \left[\frac{-1}{(K\sqrt{\bar{\rho}}\ \bar{X} - X_c)} \right] \right\} \qquad (13)$$

Here, K is a constant related to the eddy viscosity; $\bar{X}$ is the nondimensional axial coordinate expressed in jet radii; $\bar{\rho}$ is the ratio of the ambient air density to the jet exit density; and $\bar{X}_c$ is a nondimensional potential core length which has the universal value of 0.70. The parameter K varies with jet Mach number, M_0, and is assumed to be constant. The values used in this analysis are according to Witze[9] and are given by:

---

[11] *H. Schlichting, Boundary Layer Theory, 6th Edition, Chapter 24, McGraw-Hill Book Company, 1968.*

[12] *Colemans DuP. Donaldson and K. Evan Grey, "Theoretical and Experimental Investigation of the Compressible Free Mixing of Two Dissimilar Gases," AIAA Journal, Vol. 4, No. 11, November 1966, pp. 2017-2025.*

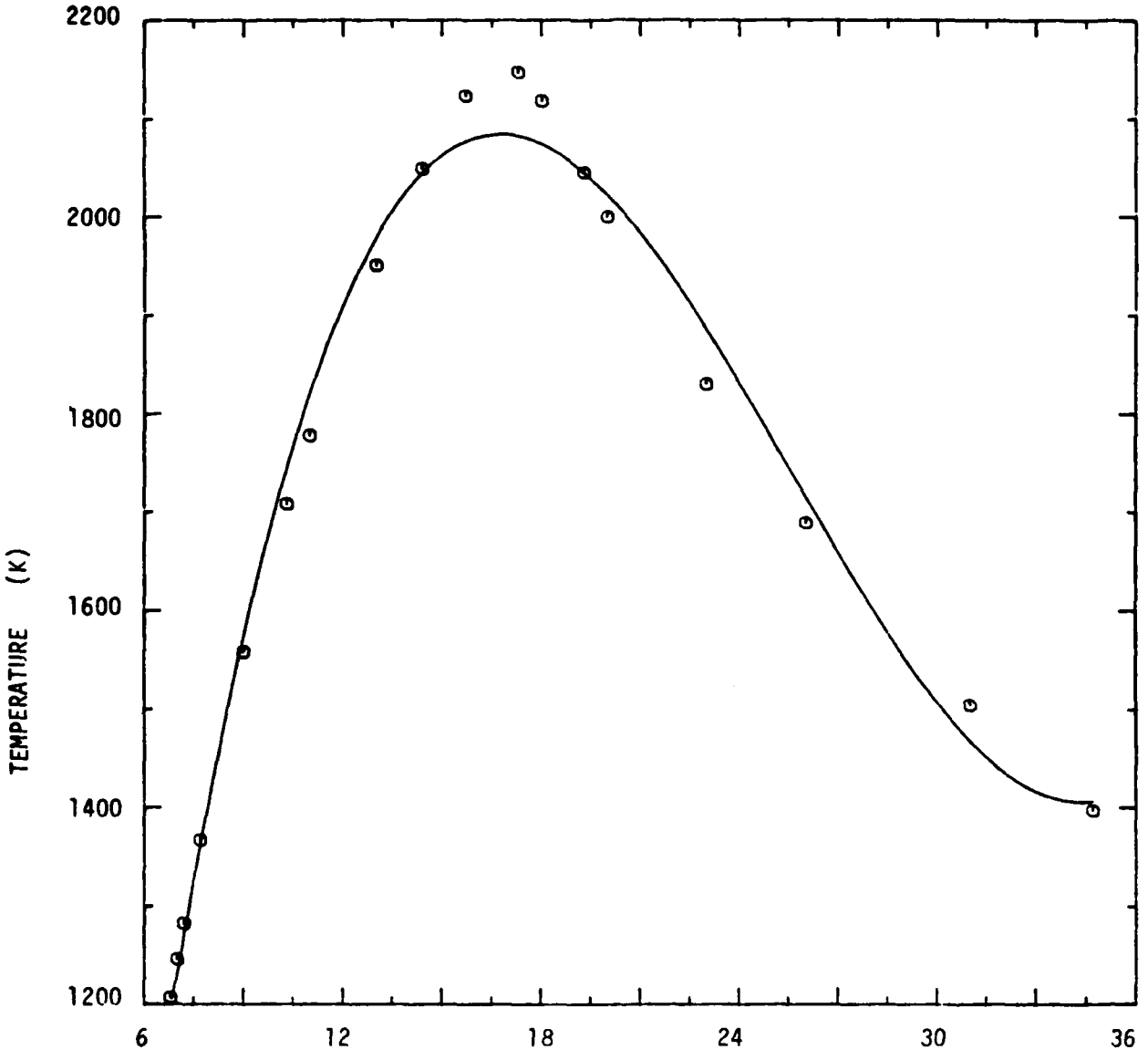

Figure 9. Effect of Mass Ratio on Flame Temperature

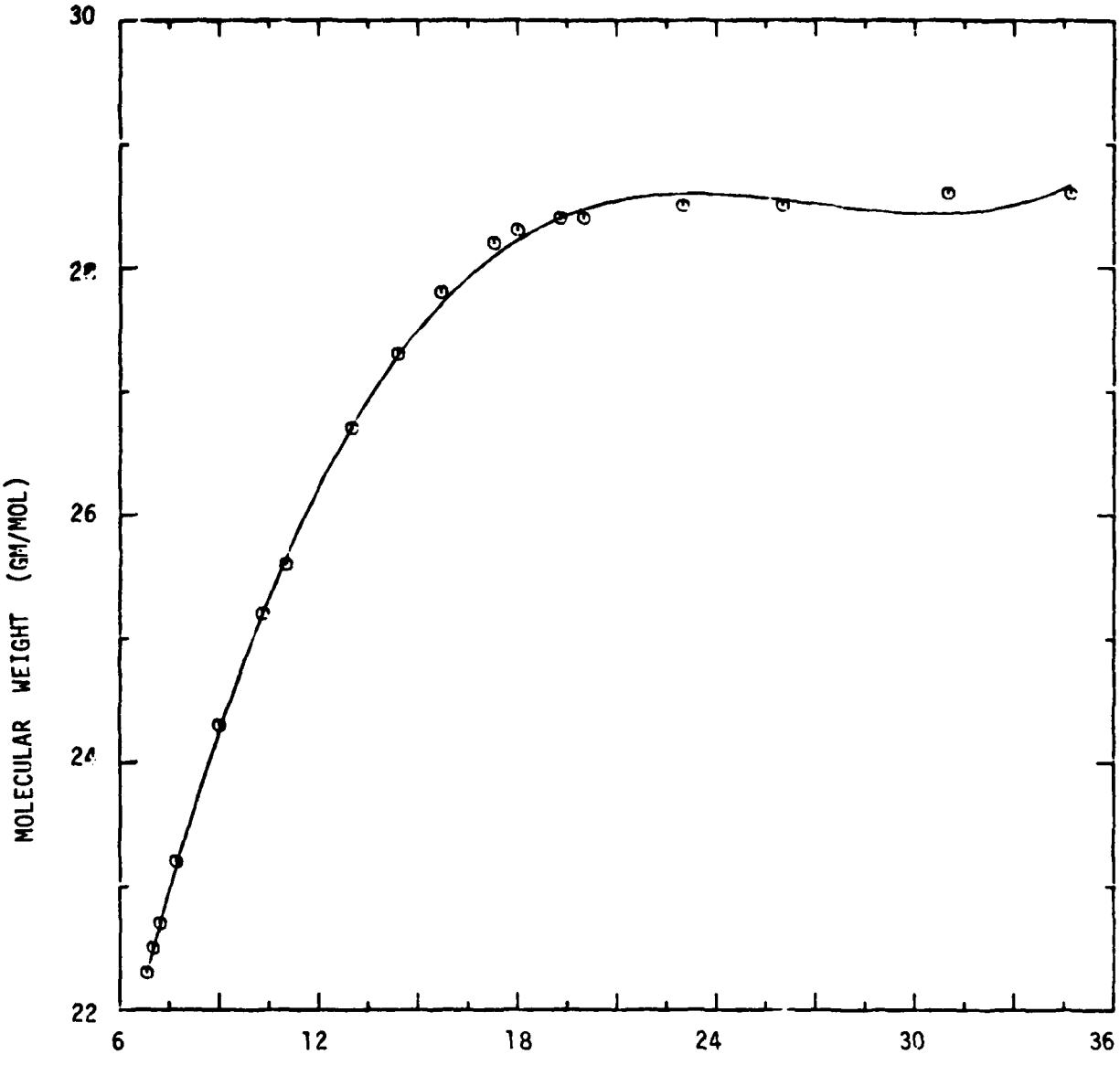

Figure 5 Effect of Mass Ratio on Molecular Weight

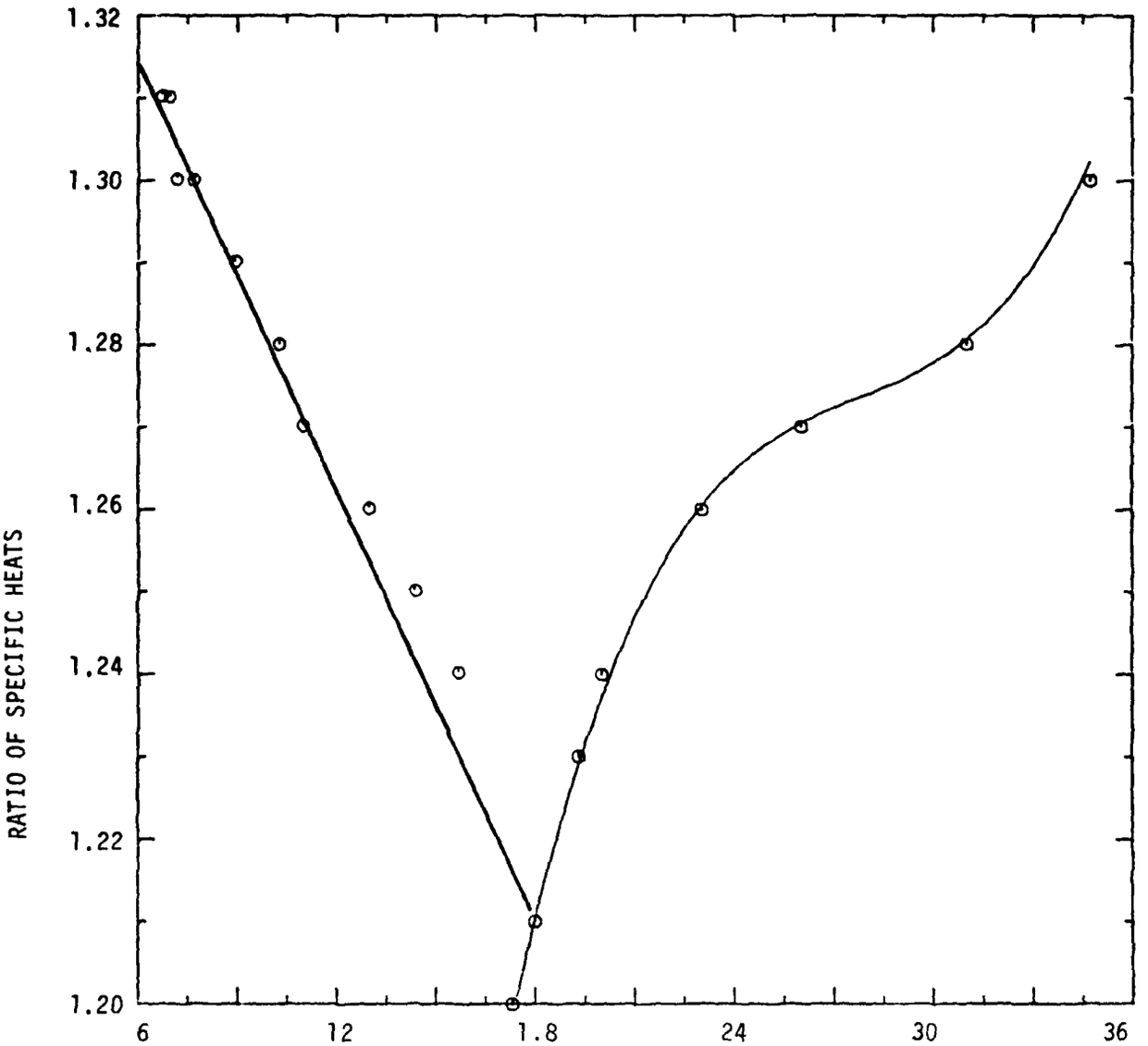

Figure 6. Effect of Mass Ratio on Specific Heat Ratio

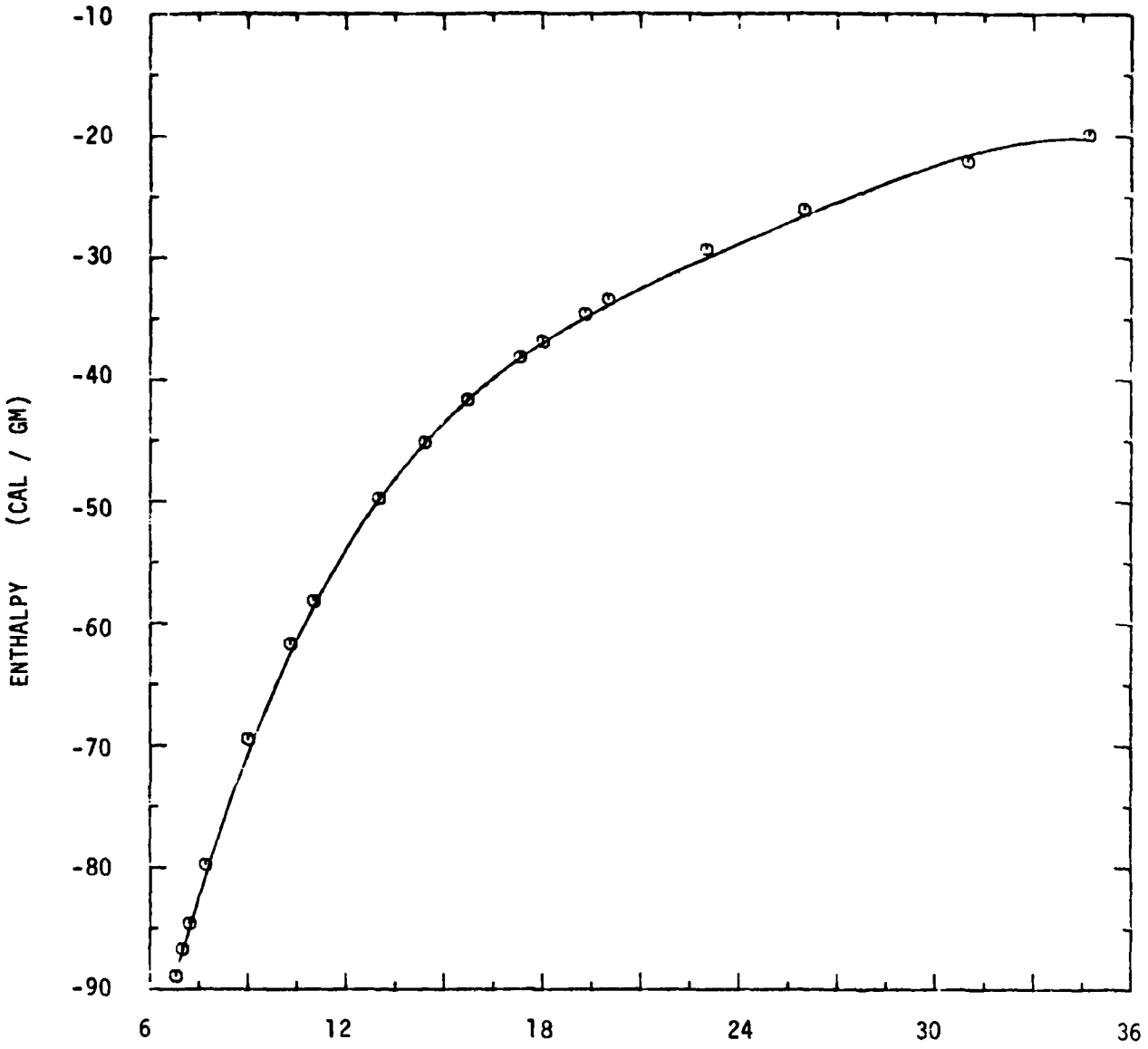

Figure 7. Effect of Mass Ratio on Enthalpy

$$K = 0.063 \left(M_o^2 - 1\right)^{-0.15} \qquad M_o > 1 \tag{14}$$

and

$$K = 0.08 \left(1 - 0.16\, M_o\right) \bar{\rho}^{-0.22} \qquad M_o \leq 1 \tag{15}$$

The jet is composed of a core region where the velocity is constant. Beyond the length of this core, the centerline velocity is given by Equation (13). Away from the centerline, i.e., in the radial direction, the velocity in the axial direction decays exponentially:

$$U(r) = U_c \exp\left[-\ell n 2 \left(\frac{r}{r_{.5}}\right)^2\right] \tag{16}$$

where $r_{.5}$ is the radial position where the velocity is one-half of the centerline velocity.

At any downstream location, the jet will spread as the centerline velocity decays. According to Kleinstein[8] the radius of the jet to the point where the velocity is one-half of U_c is:

$$r_{.5}(\bar{X}) = 0.074\, \bar{X} - 0.70\, (\bar{\rho})^{-1/2} \tag{17}$$

In addition, the total enthalpy will decay in a form similar to the centerline velocity and is given by Kleinstein[8] as:

$$\frac{H_c(\bar{X}) - H_\infty}{H_o - H_\infty} = 1 - \exp\left[\frac{-1}{(0.102\sqrt{\bar{\rho}}\,\bar{X} - 0.7)}\right] \tag{18}$$

From Equation (18), the temperature decay along the centerline may be computed from the energy equation

$$C_p T_c(\bar{X}) = H_c(\bar{X}) - \frac{1}{2} U_c^2 . \tag{19}$$

All of the estimates made in this section are based on the free jet expansion by turbulent mixing. The presence of a target downstream may influence measurements made in the vicinity of the target. Therefore, it is necessary to make an estimate of the wall influence.

It was shown by Rand[6] that the centerline velocity in the presence of a wall may be estimated by

$$U_{c_{wall}} = U_{c_{no\ wall}} \left(1 - \exp \left[-2 \left(\frac{Z}{r_o} \right)^2 \right] \right) \qquad (20)$$

where Z is the distance from the wall and r_o is the jet radius ($r_{.5}$ is a convenient value to use) if no wall had been present. Sample calculations indicate that measurements by probes 30 cm (one foot) from the wall will be influenced less than 5 percent by the wall for fuel rich mixtures. However, for very lean mixtures, the radius of the combustion products is sufficiently large for the ratio (Z/r_o) used in Equation (20) to become quite small. Under these circumstances, the influence of the wall is more significant and the core length is sufficient to engulf the probe.

The exponential form of Equation (16) is such that the maxium velocity occurs at only one point and decays to one half the maximum value at $r_{.5}$. It would appear reasonable to expect the measured velocities would be more related to the average value than the local maximum. Therefore, average velocity, $\bar{U}$, is defined over that interval where the velocity is equal to or greater than one half of the centerline velocity,

$$\bar{U}_c = \frac{2}{r_{.5}^2} \int_o^{r_{.5}} r\, U(r)\, dr \qquad (21)$$

Utilizing Equation (16), the average velocity is given by the integral

$$\bar{U} = U_c\, 2 \int_o^1 y \exp\left[-(\ell n 2)\, y^2 \right] dy \qquad (22)$$

so that

$$\bar{U} = .72\, \bar{U}_c \qquad (23)$$

This simple result will be used later during comparisons with experimentally obtained velocities and heat fluxes.

E. Heat Transfer

The purpose of the facility is to test various insulation systems suitable for use on railroad cars. In order to complete the analysis of this test configuration, the heat transfer to the target must be computed. Measurement of heat transfer is accomplished with a commercially available probe; however, some of the coefficients are dependent on geometry and flow conditions. Therefore, a brief discussion of the heat transfer to the target plate is warranted.

In choosing an appropriate analytic expression for the heat-transfer coefficient, a number of physical processes must be considered. Immediately upon leaving the orifice, and after expansion to atmospheric pressure, the jet begins to entrain air. This entrainment leads to turbulence, which is further enhanced by the combustion process. Increasing free stream turbulence has a direct effect on local heat transfer coefficients. However, for both fully developed turbulent jets and for initially laminar jets that become turbulent as a result of jet mixing (e.g., entrainment of air), the intensity of turbulence appears to be uniquely determined[13] by the jet Reynolds number and the dimensionless jet length, expressed in terms of effective orifice diameters. Thus, the data on heat-transfer rates can be correlated very effectively without any separate parameter to characterize turbulence.

The jet hits the plate and a stagnation boundary layer is formed, Figure 8. In the stagnation region, the flow field is laminar and the boundary layer is thin.[14, 15, 16] Since the boundary layer is thin, the heat-transfer coefficient can be large. It has been noticed that "... the disappearance of the pressure gradients which exist in the vicinity of the stagnation point ... serve(s) to stabilize the laminar boundary layer, in spite of locally already high turbulence levels in the free stream. Thus, it is only at the outer edge of the jet deflection region that conditions are conducive for a transition from a laminar to a turbulent boundary layer to take place."[13]

---

[13] *Robert Gordon and J. Cahit Akfirat, "The Role of Turbulence in Determining the Heat-Transfer Characteristics of Impinging Jets," Int. J. of Heat Mass Transfer, Vol. 8, 1965, pp. 1261-1272.*

[14] *James R. Welty, Charles E. Wicks, and Robert E. Wilson, Fundamentals of Momentum, Heat, and Mass Transfer, 2nd Edition, John Wiley & Sons, 1976.*

[15] *W.D. Baines and J.F. Keffer, "Shear Stress and Heat Transfer at a Stagnation Point," Int, J. Heat Mass Transfer, Vol. 19, 1976, pp.21-26.*

[16] *H. Kremer, E. Buhr, and R. Haupt, "Heat Transfer from Turbulent Free-Jet Flames to Plane Surfaces," Heat Transfer in Flames, N.H. Afgan & J.M. Beer, Ed., John Wiley & Sons, 1974.*

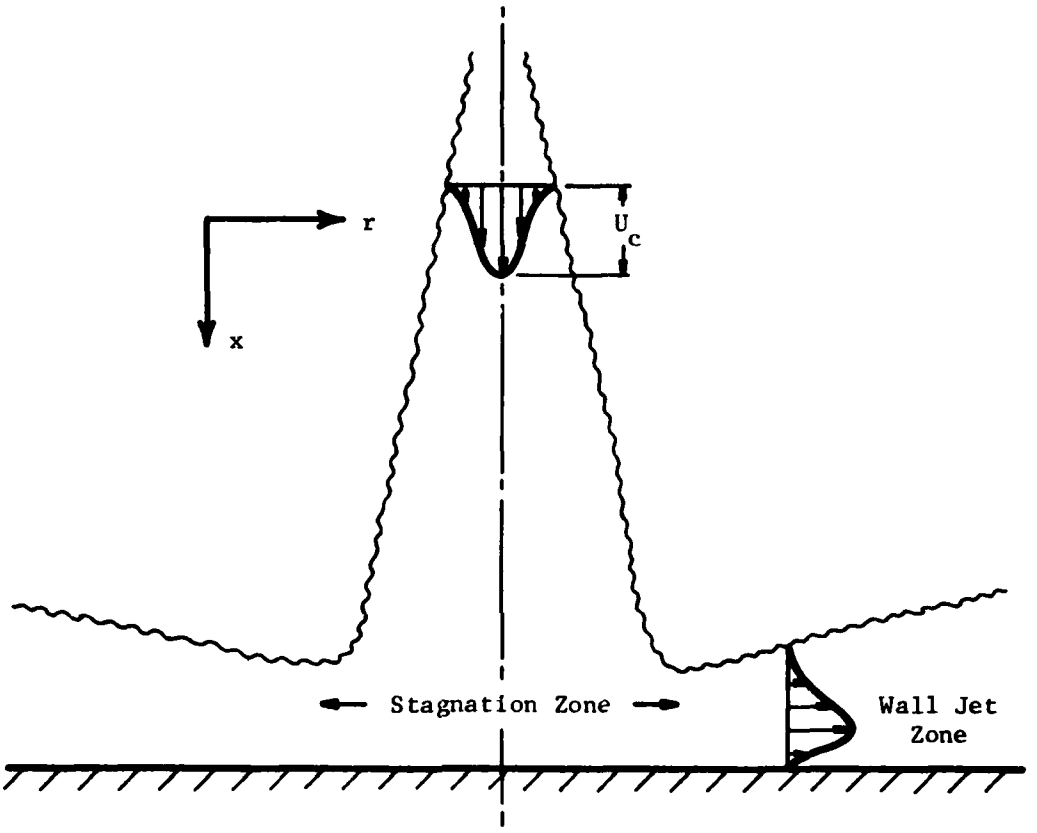

Figure 8. The Impinging Jet

In the present analytic model of a combusting propane jet interacting with a flat plate, the reaction zone is assumed to be physically separate from the jet/plate interaction. In reality, this may not be true and, therefore, an expression for chemical reactions might need to be included in the computation of the heat-transfer coefficient. However, the data from some investigators[16,17] have shown that good agreement can be obtained with experimental data even if the chemical kinetics may make the analytic prediction a worse predictor of the heat-transfer coefficient (except perhaps for a catalytic surface). These findings may be explained by the fact that the laminar boundary layer is thin; thus, the number of reactions contributing to the heat transfer in the boundary layer is very small and, therefore, can be neglected when computing the heat-transfer coefficient.

Thus, an analytic expression for the Nusselt number, Nu, in terms of the Prandtl number, Pr, and Reynolds number, Re, can be derived from laminar, stagnation flow:

$$Nu_R = \text{Constant} \cdot Pr^{0.4} \, Re_R^{0.5} \tag{24}$$

where

$$Nu \equiv hR/k \tag{25}$$

Here, h is the convective heat transfer coefficient, R is the stagnation radius, and k is the thermal conductivity of the boundary layer. The Reynolds number is computed from free stream variables, while the Prandtl number and thermal conductivity are computed using the average temperature of the free stream and wall temperatures. The constant of proportionality is dependent upon the geometry; for a three-dimensional jet of radius R impinging upon a flat plate, the constant has a value of the order of 0.5[14]. The stagnation radius, R, is taken to be the width of the jet at half-velocity, Equation (17), and the velocity used in computing the Reynolds number is the average value defined by Equation (23). The heat-transfer coefficient can then be written:

$$h = 0.45 \, k \, (U_c/R\nu)^{0.5} \, Pr^{0.4} \tag{26}$$

where ν denotes the kinematic viscosity of the fluid.

Since the stagnation radius and average velocity are dependent upon the orifice-to plate distance, it can be seen that the heat-transfer to the plate is also dependent on this distance. As the centerline velocity

[17] *R. Donnelly and R.M. Davies, "A Study of Convective Heat Transfer from Flames," Int. J. Heat Mass Transfer, Vol. 15, 1972, pp. 2155-2172.*

decreases exponentially with distance, and R increases linearly with distance, the heat transfer to the plate is obviously reduced as the plate is moved away from the orifice. From Equation (26), it is obvious that the properties of the combusting jet such as gas velocity, gas density, viscosity, flame conductivity and flame temperature (the fluid properties are temperature dependent and the heat transfer depends upon the difference in flame temperature and plate temperature) are important in computing the actual heat transfer from the jet to the plate.

Modeling assumptions, uncertainties in calculating some of the jet parameters, and difficulties in taking experimental measurements of the "torch" require that Equation (26) be altered to determine the constant of proportionality which allows the best correlation with the experimental data.

Outside the stagnation region, the convective heat transfer to the plate changes form due to the transition from laminar to turbulent flow. Thus, for the wall jet region depicted in Figure 8, the appropriate analytic expression for the convective heat transfer is for a turbulent boundary layer over a flat plate:[18]

$$Nu_R = 0.0288\ Re_R^{4/5}\ Pr^{1/3},\quad r > R \tag{27}$$

where, now, the Nusselt and Reynolds numbers are a function of the radial distance from the stagnation point. The wall jet velocity decays according to:

$$U_r = \bar{U}\ \left\{1 - \exp\left[-2\left(\frac{r}{2R}\right)^2\right]\right\}^{1/2} \tag{28}$$

Hence, the heat transfer coefficient can be computed:

$$h = 0.0243\ \frac{k}{R}\left(\frac{RU_c}{\nu}\right)^{4/5}\ Pr^{1/3}\ \left\{1 - \exp\left[-2\left(\frac{r}{2R}\right)^2\right]\right\}^{4/10}\quad r > R \tag{29}$$

Again, due to uncertainties in various parameters, the constant of proportionality is altered for the best correlation with experimental data. The

[18] *James R. Welty, Engineering Heat Transfer, John Wiley & Sons, 1974.*

heat flux to the plate, $\dot{q}$, consists of a convective and radiative component, and can be written as:

$$\dot{q} = h_r(T_F - T_P) + \sigma\varepsilon_p\varepsilon_F\ (T_F^4 - T_P^4) \qquad (30)$$

Here, the subscripts F and P refer respectively to the flame and plate; ε are their respective emissivities; σ is the Stefan-Boltzmann constant. The radiation exchange between the flame and the plate is approximated by the radiation exchange between two infinite plates. The flame emissivity is a function of quality - for a predominately liquid flame (quality $\sim$ 0), ε_F approaches 1.0 because the fuel rich propane/air mixture produces considerable radiation.[19] For the diffusion flames, it has been noted that the tendency for carbon and soot formation increases with mass flow and for very fuel rich flames which results in a larger radiative component. The flame is optically thinner for a "vaporous" flame and the radiative component to the heat transfer is substantially reduced.

In summary, the heat transfer from the burning propane torch to the plate consists of a radiative and convective component, Equation (30), where the convective component is given by:

$$h_r = \alpha \frac{k}{R} (U_c R/\nu)^{0.5}\ Pr^{0.4} \qquad r \le R \qquad (31)$$

$$h_r = \beta \frac{k}{R} (U_c R/\nu)^{0.8}\ Pr^{0.33} \left\{ 1 - \exp\left[2 \left(\frac{r}{2R}\right)^2 \right] \right\}^{0.4} \qquad r > R \qquad (32)$$

where α and β are found from correlation with the experimental data.

In the experiments performed by the BRL, a calorimeter manufactured by Thermogage was placed approximately along the centerline of the torch. The sensing element is in the tip of a cone where the apex of the cone has been "rounded," and has a radius of approximately 0.32 cm. In order to compare the experimental data with the theory, the heat-transfer coefficient of the torch to the Thermogage probe must be estimated. Equation (31) is applicable but the constant must now be evaluated for the geometry of the probe. The result of this analysis yields:

---

[19] *A. G. Gaydon and H. G. Wolfhard, Flames, Their Structure, Radiation and Temperature, 4th Edition, "A Halsted Press Book," John Wiley & Sons, 1979.*

$$h_{torch \rightarrow probe} = 1.07 \, (U_c / R_{probe} \, \nu)^{0.5} \, P_r^{0.4} \qquad (33)$$

where $R_{probe} = 0.32$ cm.

F. Parametric Analysis

The analysis procedures described here have been programmed for the purpose of rapid numerical evaluation.[5] The results shown in Figure 2 are typical of the flow properties at the exit of the orifice. It may be seen that the jet exit velocity is a strong function of reservoir quality and pressure.

The results of the combustion analysis indicated that the most significant thermodynamic property is flame temperature. This property is most sensitive to the mass ratio of air to fuel and relatively insensitive to other parameters such as reservoir pressure or quality.* Since the target is engulfed in the jet formed by the combustion products, and since these properties are independent of quality, the computed flow conditions (per our modeling assumptions) at the target are also independent of quality.

A parametric study was conducted for the mass ratios and reservoir pressures of interest assuming a quality of one (pure vapor). Although many flow properties are computed, the temperature and the heat flux at the probe in front of the target are typical. These results are presented in Figures 9 and 10 and graphically demonstates the insensitivity of these results to reservoir pressure.**The points on these figures represent pressures between 0.827 and 1.65 MPa (120 and 240 psia) which spans the region of interest at the torch simulation facility.

Another result of this parametric study was the observation that for large mass ratios, the core length of the jet formed by the combustion products was sufficiently long to engulf the measuring probe. This effect is observed for fuel lean mixtures and is caused by the addition of large quantities of air which slows the original propane jet and increases the radius of the mixture to the point that the core length predicted by diffusion theory exceeds the distance to the target. Therefore, the reduced temperatures shown in Figure 10 are more indicative of an excess of air during combustion than cooling during the diffusion process.

This model assumes a simplified mixing theory where the fuel and air are thoroughly mixed before combustion. With this assumption, the flame temperature was found to be essentially independent of quality. A more detailed, two-dimensional analysis would be required to account for the two-phase mixture across the width of the jet.

**Note that for air-to-fuel ratios greater than stoichiometric, that the temperature is virtually independent of pressure, and is relatively insensitive to pressure for ratios lower than stoichiometric.*

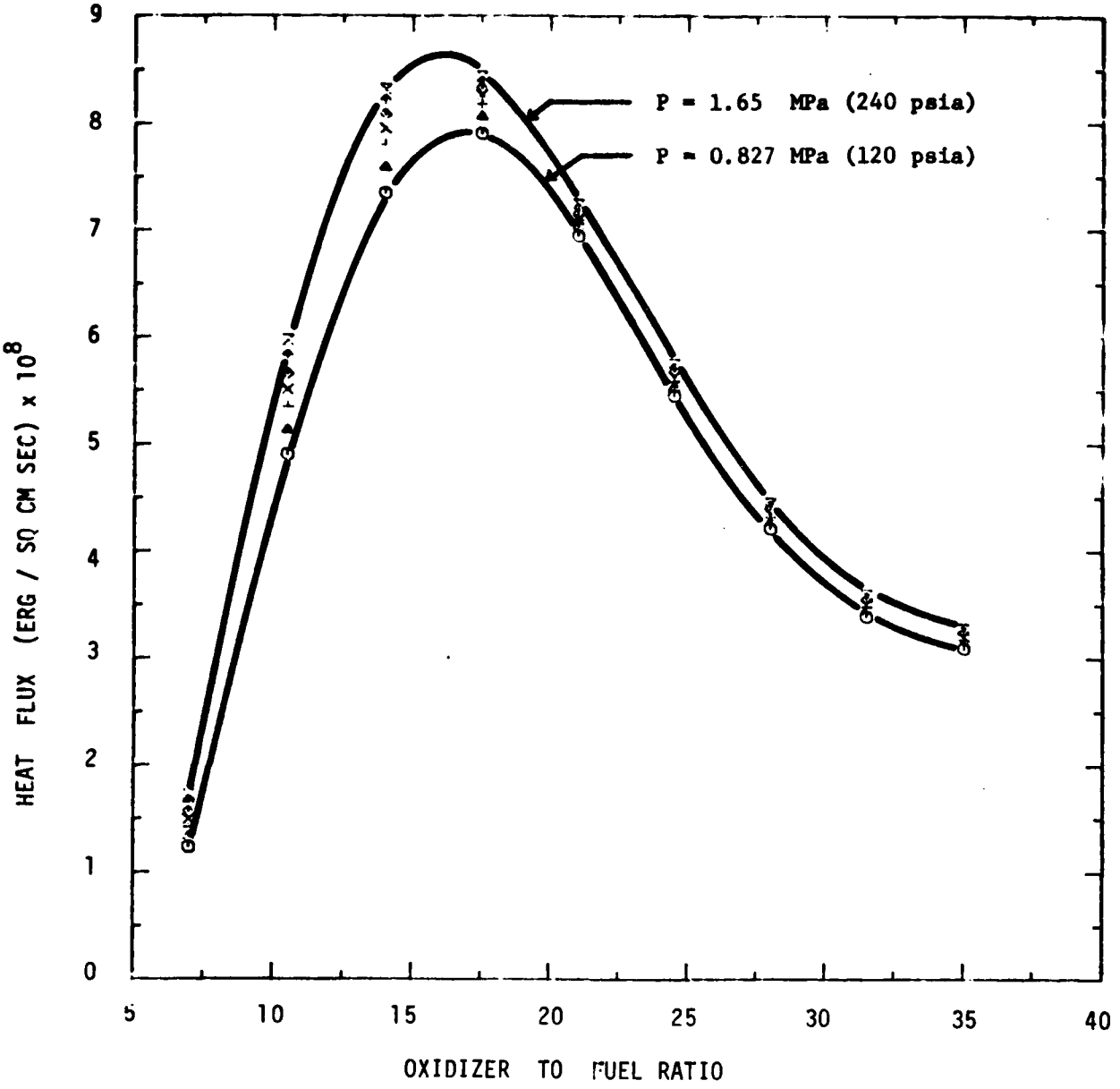

Figure 9. Effect of Mass Ratio on Heat Flux for Various Pressures

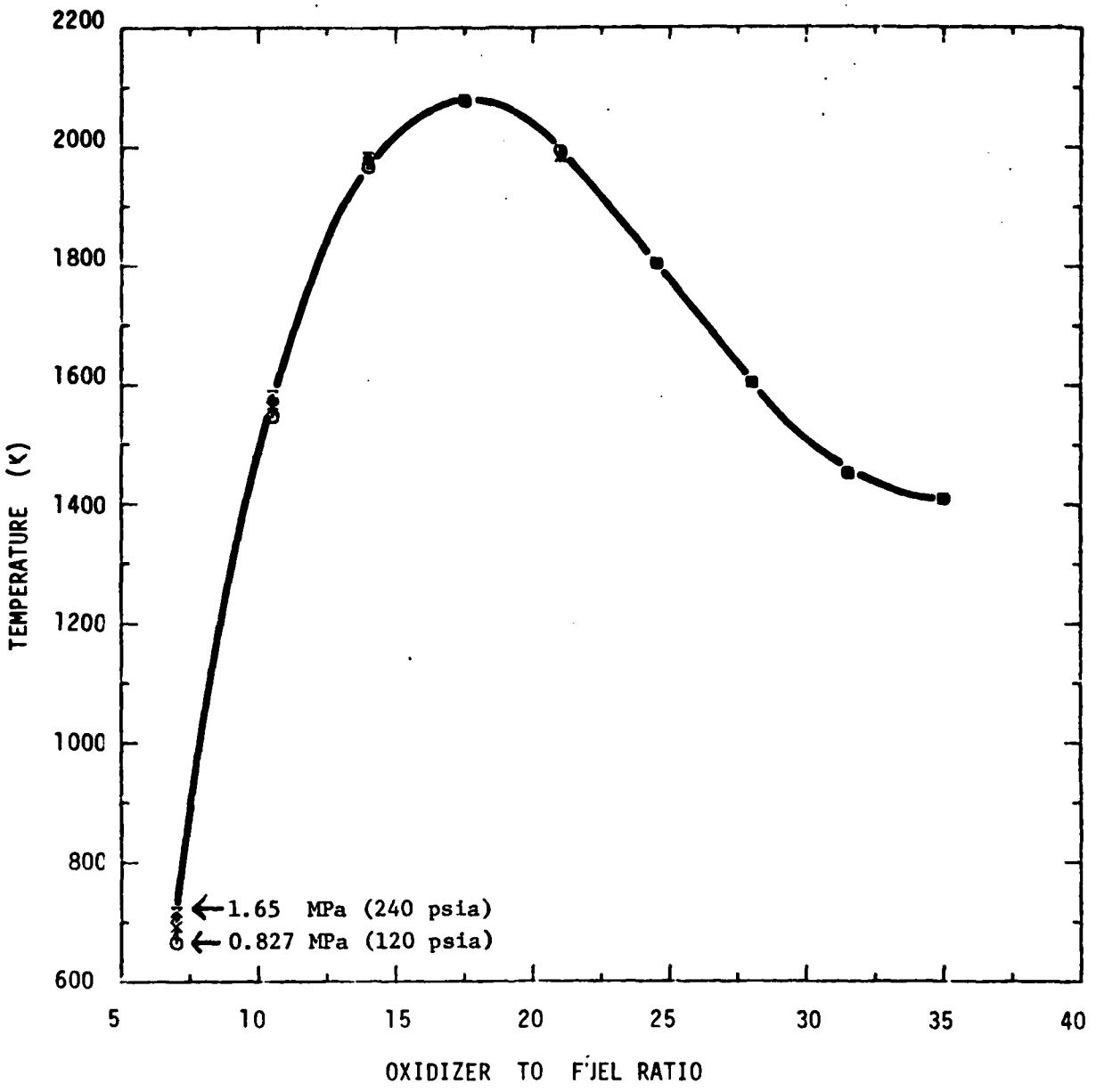

Figure 10. Effect of Mass Ratio on Temperature for Various Pressures

III. DATA ANALYSIS

A series of tests were conducted at the torch simulation facility in Pueblo, Colorado, from 28 October to 2 November 1978. The configuration was as depicted in Figure 1. Valves A and B were electrically driven, manually controlled gate valves that were intended to control the quality of the effective reservoir upstream of the orifice. The target was instrumented with a number of Tempellets positioned just in front of a steel plate; a Hastings velocimeter probe and a Thermogage calorimeter were centered 30 cm in front of the plate. Analog data were taken as a function of time, converted to digital signals and recorded. Data were taken indicating both valve rotation positions, pressure upstream of the orifice, velocity and heat flux at the probe position. The recorded data from 13 tests have been collected and are contained in Appendix A of this report.

The purpose of this study is to compare the analytic model predictions to measured experimental quantities. The data contained in Appendix A is assumed to be accurately measured and calibrated. An attempt has been made to estimate the uncertainty of the heat flux measurements due to the fluctuating nature of the torch. This estimate was made by analyzing the high frequency variability of the data.

A. Valve Data

Two identical valves were used to control the flow of propane to the orifice. Valve A controlled the liquid phase and valve B the vapor phase. These valves have a two inch diameter orifice and are positioned in a four inch line. It was recognized that some rotation of the valve was necessary before any flow could occur due to the design of the valve. It was also recognized that as the valve was rotated and the flow increased, a point would be reached where the small nozzle at the exit of the manifold would choke the flow and allow the measured pressure to approach the tank pressure. Further rotation of the valve would not influence the measured pressure or any other flow parameter.

No calibration data was supplied with the experimental records so that there is no way to directly compute the quality of the reservoir from the recorded valve positions. However, a study of the records in Appendix A revealed that a number of tests were conducted with the liquid valve, A, in the completely closed position. These four tests, 147, 148, 149, and 150, were examined in detail to obtain the valve opening characteristics. All data is scaled to values between zero and one thousand for convenience in presentation. In the case of a valve, this scale corresponds to rotation angles from zero to 90°. The pressure is measured just upstream of the exit nozzle which has an orifice diameter of 0.95 cm. The controlling valves have a maximum orifice size of approximately 5 cm when fully opened. When the valve is sufficiently open, the measured pressure will be the tank supply pressure and the exit nozzle will serve to limit the flow.

In order to assess the effectiveness of valve rotation, the ratio of the measured pressure upstream of the exit nozzle and the tank supply

pressure is shown in Figure 11 as a function of measured valve rotation. The data was taken from tests 147 through 150 during which the liquid valve was completely closed. The pressure response of Valve B is surprisingly linear with valve rotation. Of particular interest, at positions below 176, the valve may be considered completely closed. Also, at positions above 410, the valve is open sufficiently for the tank pressure to be measured at the exit nozzle. This observation is significant in that certain conclusions can be drawn about the quality of the reservoir conditions.

Valve A which controls the flow of liquid propane to the nozzle exit is identical to valve B. Due to the difference in densities between liquid and vapor at high pressures, the onset of flow through valve A should require the same or slightly larger rotation than valve B. Therefore, at valve settings below 176, no liquid is being supplied to the manifold and the resulting reservoir upstream of the nozzle exit is supplied by the saturated vapor supply only.

An examination of the experimental records contained in Appendix A indicates that in the majority of cases, the liquid valve may be considered to be completely closed and the vapor valve completely open. Only tests 141 and 146 indicate that valve A was open sufficiently to provide any flow of liquid. Therefore, the analysis used for comparison with experimental data have an assumed quality of one.

B. Velocity and Calorimeter Data

At this point, it is appropriate to review a typical experimental record to understand the manner in which the data will be examined. Test 137 is typical and will be discussed in detail. The relationship between the various symbols shown and the values plotted is given at the beginning of the Appendix. The five quantities measured were: A, the liquid valve opening; B, the vapor valve opening; G, orifice pressure (psig); N, the heat flux (Btu/ft^2 sec); and O, the velocity (ft/min at standard temperature and pressure).

The initial conditions indicated on this record are as follows:

Quantity	Value	Remarks
A	125	Rotated 11.25° - no flow
B	410	Rotated 36.9° - fully open
G	0	Indicates no fuel at orifice; valve C (Figure 1) probably closed
N	0	No heat transfer indicates either no flow or no ignition of mixture
O	150	Velocity measured is 300 ft/min (2.96 knots). This corresponds to the observed

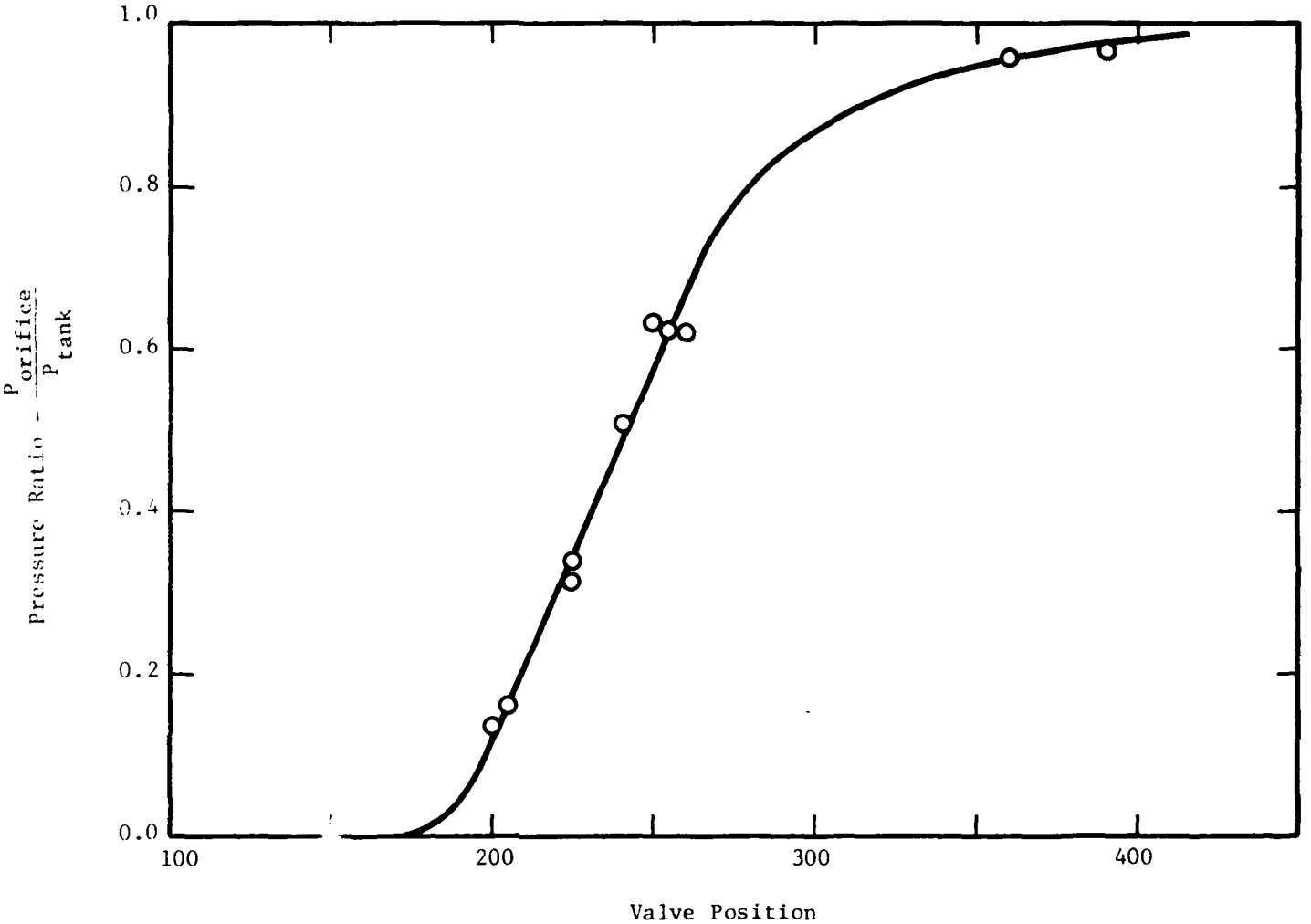

Figure 11. Vapor Valve Response

wind conditions at the time in the direction of the target

At 1.2 minutes into the test, valve C is opened as evidenced by the sudden increase in orifice pressure. Significant increase in measured velocity is indicated but without heat transfer. Flow is obviously an unignited mixture of propane and air.

At 3.5 minutes into the test, valve C is closed and at 4 minutes the data recorder is interrupted and then restarted at 9.5 minutes. At 10.1 minutes, valve C is again opened and mixture ignited. Both velocity and heat flux are shown to be fluctuating with peak values of 1540 ft/min and 43.5 Btu/ft^2-sec respectively. The test is terminated after 14.5 minutes by closing valve C.

Each record must be examined individually to extract meaningful information. The velocity measuring device has a relatively slow response time so that fluctuations are generally considered to be an integrated effect of locally turbulent conditions caused by a variety of sources including gusting winds. The peak values are of most significance and are listed in Table 2. In some tests, the flow conditions were changed during the course of the test. Therefore, multiple data points are listed in those cases. The calorimeter data shown in the experimental records appears to be the RMS value of the analog data.[20] The fluctuations in the analog data are of a relatively high frequency with a peak to peak amplitude on the order of 20 percent of the mean value. Both velocity and heat flux data have been converted to cgs units so that direct comparison with the analysis contained in Section II is possible. These dimensional values are also listed in Table 2.

IV. RESULTS AND DISCUSSION

In order to predict the velocity and heat flux at the target using the analysis procedures contained in Section II, it is necessary to have some knowledge of the mass ratio of air to propane. This parameter dominates the combustion process which in turn controls the downstream flow properties. The theoretical results already presented as Figures 9 and 10 are replotted as a function of reservoir pressure for various mass ratios in Figures 12 and 13. In this form the experimental values contained in Table 2 may be presented since both ordinate and abscissa are measured quantities.

The velocity data contained in Table 2 is superimposed on the analysis results in Figure 12. Different symbols have been used to identify those data obtained with the liquid valve completely closed. It can be seen from this figure that all usable data falls within a relatively

[20] *Charles Anderson, private communications.*

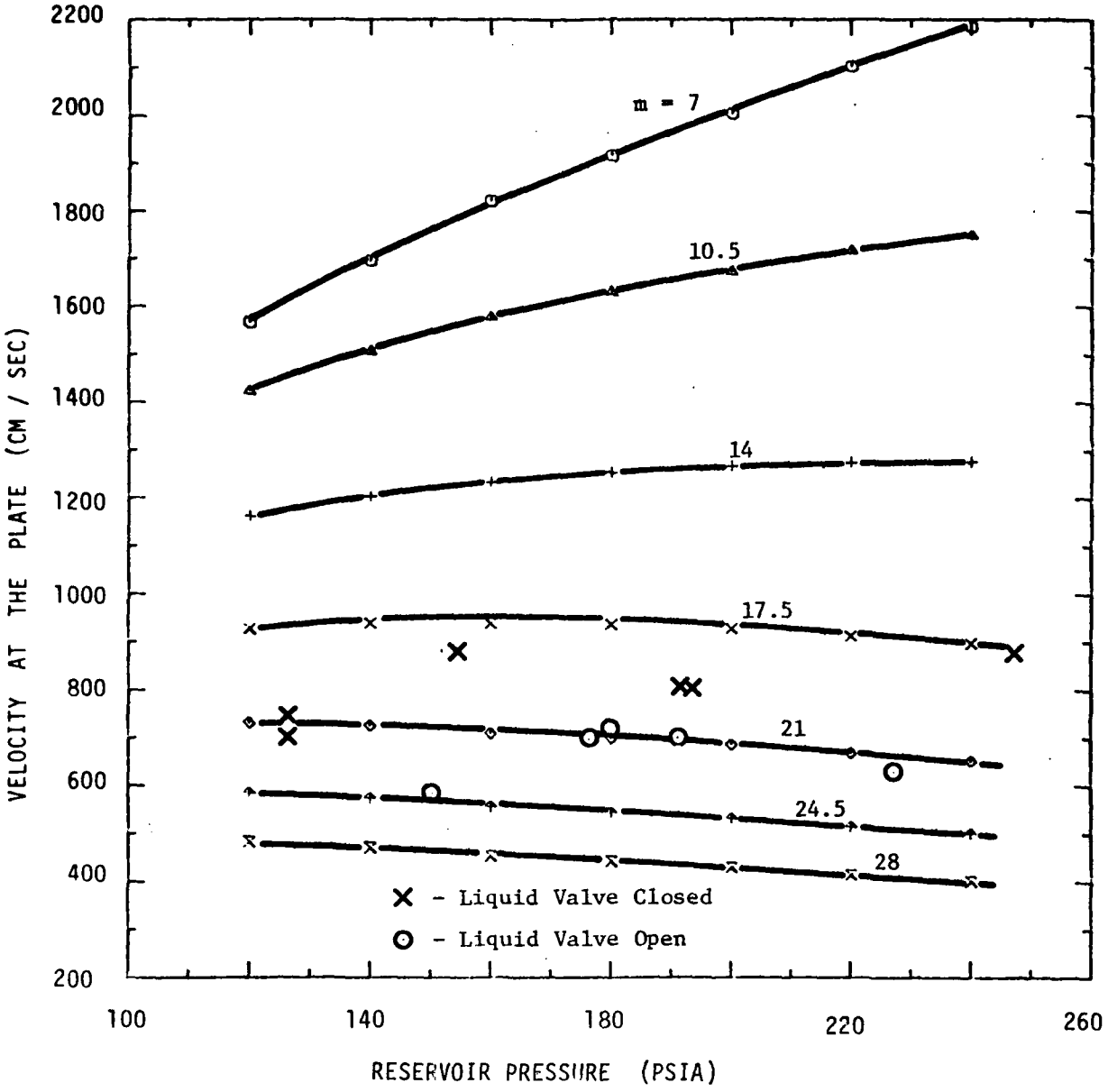

Figure 12. Effect of Reservoir Pressure on Average Velocity at Plate

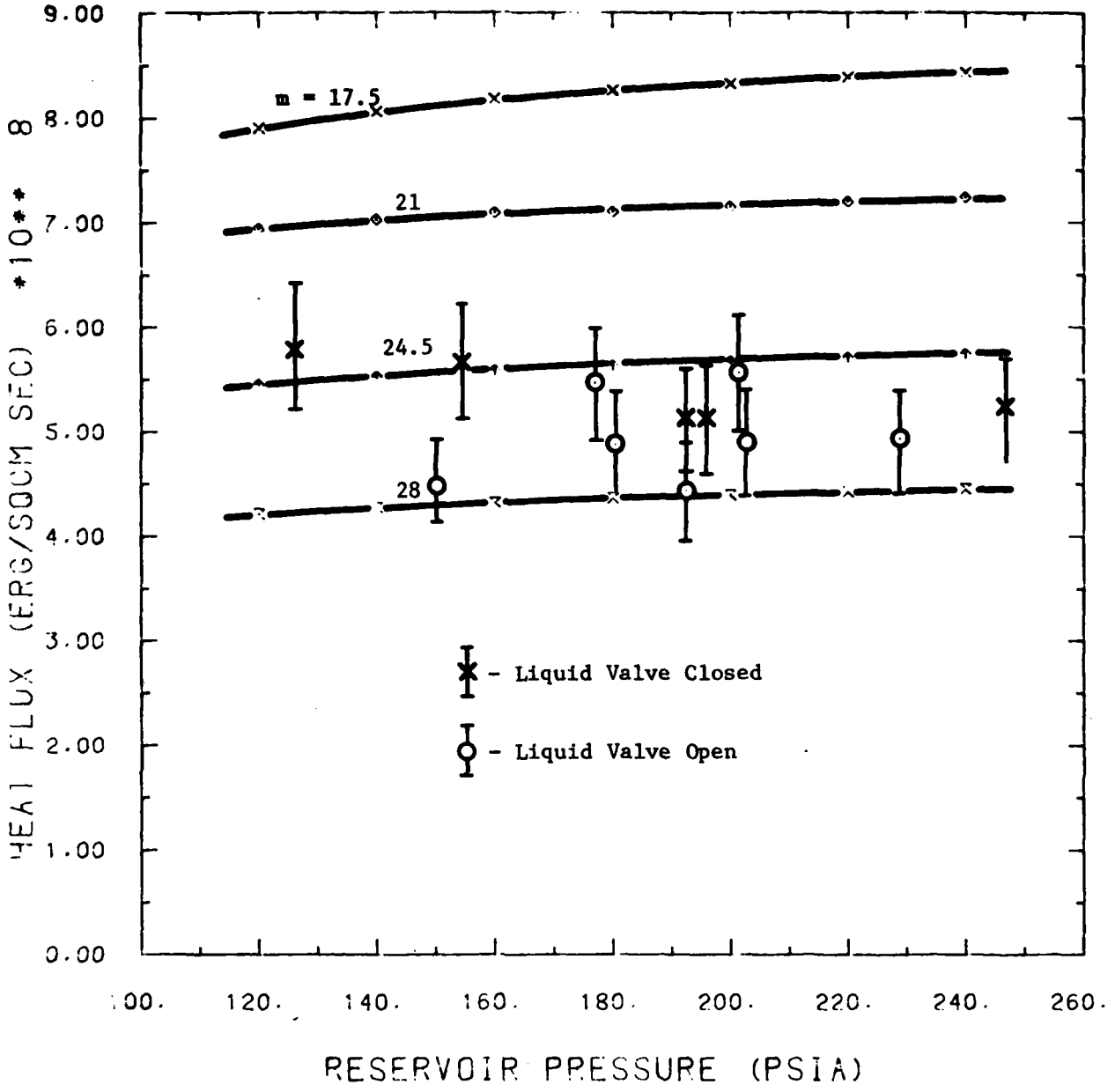

Figure 13. Effect of Reservoir Pressure on Heat Flux to Probe

narrow band bounded by mass ratios from 17.5 to 24.5. At the inception of this program, it was expected that combustion would occur first with a fuel rich mixture which is represented by mass ratios less than 17.3. However, the data suggests that combustion occurs in this facility only with a lean mixture. In practice, the combustion of a fuel jet is actually a two-dimensional phenomenon. Ignition probably occurs at the periphery of the jet where lean mixture exists. Once ignited, the flame may propagate to the centerline so long as the mixture is sufficient to support combustion. The one-dimensional measurement of flow properties is actually a measurement of the integral effect over the width of the jet. For lean mixtures, the assumption of thorough air-fuel mixing before combustion appears to be a relatively valid approximation (i.e., comparison of analytic predictions with the experimental data). Thus, the validity of the complete mixing-before-combustion assumption, along with the integral effect, allow a one-dimensional fuel lean mixture model to yield realistic predictions.

Since the data obtained from those tests with the liquid valve completely closed does not overlap the other data, it may be concluded that a high quality flow such as that produced by a saturated vapor source will burn closer to stoichiometric condition than more fluid flames. The balance of the data suggests that the addition of very little liquid will increase the mass of air required for combustion disproportionately. The theoretical observation that the resulting flow parameters are relatively independent of reservoir pressure is confirmed by the experimental observations.

The variability in the peak velocity data is well within the expected range of scatter due to wind gusts and the difficulty in aiming the propane source. Bouyancy effect of the flame coupled with less than ideal wind conditions make it very difficult to center the point of impingment within a circle of radius 8 cm at a distance of 365 cm. This is the radius of the theoretical half velocity point under stoichiometric conditions. Unfortunately, the variability of this data is sufficient to mask any subtle effects of pressure. At the same time, the data indicates that the mass ratio is influenced by very small changes in the liquid valve setting.

The calorimeter data contained in Table 2 are superimposed on the analytic results in Figure 13. In addition, an error bar has been included which is $\pm$ 10 percent of the measured flux. This is based on the fact that analog data indicates an oscillation of this order of magnitude. In this figure, only theoretical results for fuel lean mixtures are presented. These results are dependent of the radius of the probe which was estimated to be 0.32 cm. Theoretical agreement could be obtained by increasing this number slightly; however, in the absence of details of the probe, these results are considered adequate to explain the heat transfer mechanism. The experimental data does not seem to support the reduction in heat flux for increased mass ratios. This is believed to be due to the increase in emissivity with increasing amounts of fluid. This feature has been reported by observers but has not been taken into account in the analysis.

Table 2. Torch Simulation Data

Test	Tank Pressure (psig)	Liquid Valve	Vapor Valve	Orifice Gauge	Pressure (psig)	Initial Velocity	Peak Velocity (ft/min)	Peak Velocity (cm/sec)	Heat Flux BTU / Ft² sec	Heat Flux Ergs / cm² sec
TFC137	238	130	410	685	(228)	150	770	630	435	4.938 E8
TFC138	210	120	400	610	(203)	100	655	564	430	4.881
TFC139	150	130	400	450	(150)	160	740	589	395	4.484
TFC140*	168	130	400	465	(155)	150	620	478	400	4.541
TFC141*	150	200	620	480	(160)	230	760	538	435	4.938
TFC142	175	130	410	540	(180)	120	830	721	430	4.882
TFC143	176	120	395	530	(177)	50	740	701	480	5.449
TFC144	268	130	400	605	(202)	50	730	691	490	5.563
TFC145	202	0	390	585	(195)	70	865	808	450	5.108
TFC146	-	180	335	575	(192)	170	865	706	390	4.427
TFC147	200	0	360	575	(192)	60	865	818	450	5.108
TFC148	200	0	250	380	(127)	-	725	736	510	5.790
TFC149	200	0	200	80	(27)**	0	300	305	215	2.441
		0	225	205	(68)**	0	600	610	480	5.449
TFC150	250	0	205	120	(40)**	0	405	411	410	4.654
		0	224	235	(78)**	0	-	-	-	-
		0	240	380	(127)	0	680	691	510	5.790
		0	260	465	(155)	0	860	874	500	5.676
		0	1000	740	(247)	0	865	879	460	5.222

* Torch observed to be off center.
** Pressures below region of interest.

As in the case of the velocity measurements, a certain amount of variability in the data may be attributed to the aim of the propane jet and local wind conditions. In any event, the experimental data suggest that the analytic model can predict the incident velocity, heat flux and temperature of a reacting propane jet with a quality near one.

V. RECOMMENDATIONS

The experimental data from the torch simulation facility has provided the necessary evidence that the thermodynamic and fluid dynamic models developed are representative of the tests. The analysis may be used to identify where the experiment may be improved and the experimental data suggests where certain improvements in the analysis are possible.

The torch simulation facility may be improved by noting the sensitivity of the data to the mass ratio. Although the combustion process is relatively independent of pressure and quality, the mass ratio appears to be a strong function of the liquid injected into a saturated vapor flow. Therefore, better metering of the liquid is necessary if more precise information is desired from this test. This would require a new valve or precision orifices to be installed in place of valve A, Figure 1.

Much of the variability in the data is caused by the inability to center the jet downstream due to buoyance and wind effects. These effects could be reduced somewhat by conducting bench scale testing in an enclosed environment. However, there is no evidence to indicate that scaling of turbulent diffusion flames is feasible.

The model has assumed thorough mixing of the propane and air before combustion. Since the model makes predictions which are in agreement with experimental data, this assumption appears to be supported. However, the experimental data is for initial qualities near 1.0, i.e., essentially vapor flow with a small amount of liquid. For thorough mixing, the two-phase analysis indicated that the flame temperature is virtually independent of quality. Observations of the test clearly indicate that for initial qualities near zero i.e., essentially liquid flow that the combustion process is definitely two-dimensional; it is a function of radial distance from the jet centerline and axial distance from the orifice. A non-burning core of propane is clearly evident for small qualities.

Additionally, the torch radiates significant amounts of energy when the initial quality is zero. This is certainly due to incomplete combustion processes in a fuel rich zone creating carbon particles (soot) which can radiate large amounts of energy. Indeed, a "liquid" flame impacting a flat plate transfers significantly less heat to the plate compared to the "vapor" flame, indicating a combination of a cooler effective flame temperature and radiative heat losses due to the incomplete combustion processes.

The analysis could be improved by allowing the emissivity to be a function of mass ratio. This could be accomplished by measuring the radiation as well as the heat flux to a calorimeter. In the present analysis, the emissivity is assumed to be constant; however, as more fluid is added, the increase in radiant heat is quite apparent to personnel at the facility. The heat flux due to convection is reduced as the velocity is decreased with increasing fluid. However, if the radiant energy released increases, the net measured heat flux would be the sum of the two components and would be less sensitive to increases in mass ratio for small changes of quality than the present analysis indicates.

In addition, an analysis of the mixing process could be performed using a two-dimensional code (e.g., GENMIX[21]) to examine the effects of quality on the mixing process. An expected result would be that the effective flame temperature, and consequently the heat transfer, would be found to be dependent upon the quality.

Further, the analysis here only considered one location, 3.66m (12.0 ft), downstream from the orifice. Data at other locations would be required to ascertain the predictive ability of the present model at other downstream locations.

In conclusion, it has been shown that the analysis techniques developed in this program are sufficiently accurate to predict the observed phenomenon for the limited range of an initial quality near one. The torch facility is generally used with a quality near one, thus, this restriction is not too severe. To fully understand the torching mechanism for various qualities, additional data is required to establish the mass ratio as a function of liquid valve position; and an analysis of the aforementioned effects of mixing, combustion, and emissivity are required. For the data available, the mass ratio varies from 17.3 (stoichiometric) to approximately 21 when the liquid valve is in the 12 percent position and the vapor valve is in the 40 percent position. There is no reason to believe that this relationship is linear and a carefully planned series of tests is warranted to provide the necessary information to characterize the flow condition.

---

[21] *D. Brian Spalding, GENMIX: A General Computer Program for Two-Dimensional Parabolic Phenomena, Pergamon Press, Elmsford, NY, 1977.*

REFERENCES

1. Charles Anderson, William Townsend, John A. Zook, Gregory Cowgill, *The Effects of a Fire Environment on a Rail Tank Car Filled with LPG*, BRL R 1935, USA Ballistic Research Laboratories, Aberdeen Proving Ground, MD, September 1976. (AD B015605L)

2. Charles Anderson, William Townsend, John Zook, Gregory Cowgill, *The Comparison of Thermally Coated and Uninsulated Rail Tank Cars Filled with LPG Subjected to a Fire Environment*, Report No. FRA-OR8 D 75-32, National Technical Information Service, Springfield, VA, December 1974.

3. William Townsend and Richard Markland, *Preparation of the BRL Tank Car Torch Facility at the DOT Transportation Test Center, Pueblo, Colorado*, BRL unpublished report, USA Ballistic Research Laboratories, Aberdeen Proving Ground, MD, September 1975.

4. Charles Anderson, William Townsend, Richard Markland, John Zook, *Comparison of Various Thermal Systems for the Protection of Rail Tank Cars Tested at the FRA/BRL Torching Facility*, BRL unpublished report, USA Ballistic Research Laboratories, Aberdeen Proving Ground, MD, December 1975.

5. A more complete description of the modeling is given in *An Analytical Model of a Two-Phase Propane Combusting Jet*, James L. Rand, Report 02-5045-001, Southwest Research Institute, San Antonio, TX, November 1980.

6. Spalding, D.B., *A Simple Model on the Rate of Turbulent Combustion*, Turbulent Combustion, Progress in Astronautics and Aeronautics, Vol. 58, AIAA, 1978, pp. 105-116.

7. Astleford, W. J. and Dodge, F. T., *Response of Fuel Targets to Munitions: Heat Transfer Analusis of Torches Impinging on Plates*, SWRI Report No. 02-3669, June 1977

8. Kleinstein, G., *Mixing in Turbulent Axially Symmetric Free Jets*, J. Spacecraft & Rockets, 1, July-August 1964, pp.403-408.

9. Witze, P., *Centerline Velocity Decay of Compressible Free Jet*, J. Spacecraft & Rockets, 12, April 1974, pp 417-418.

10. Gordon, S. and McBride, B.J., *Computer Program for Calculation of Complex Chemical Equilibrium Composition, Rocket Performance, Incident and Reflected Shocks, and Chapman-Jouguet Detonations*, NASA Lewis Research Center, NASA SP-273, March 1976.

11. H. Schlichting, *Boundary Layer Theory*, 6th Edition, Chapter 24, McGraw-Hill Book Company, 1968.

12. Colemans DuP. Donaldson and K.Evan Grey, *Theoretical and Experimental Investigation of the Compressible Free Mixing of Two Dissimilar Gases,* AIAA Journal, Vol. 4, No.11, November 1966, pp.2017-2025

13. Robert Gordon and J. Cahit Akfirat, *The Role of Turbulence in Determining the Heat-Transfer Characteristics of Impinging Jets,* Int. J. of Heat Mass Transfer, Vol. 8, 1965, pp.1261-1272.

14. James R. Welty, Charles E.Wicks, and Robert E.Wilson, *Fundamentals of Momentum, Heat, and Mass Transfer,* 2nd Edition, John Wiley & Sons,1976.

15. W. D. Baines and J. F. Keffer, *Shear Stress and Heat Transfer at a Stagnation Point,*, Int, J.Heat Mass Transfer, Vol.19,1976, pp.21-26.

16. H. Kremer, E.Buhr, and R.Haupt, *Heat Transfer from Turbulent Free-Jet Flames to Plane Surfaces,* Heat Transfer in Flames, N.H.Afgan & J.M.Beer, Ed., John Wiley & Sons, 1974.

17. R. Conolly and R.M.Davies, *A Study of Convective Heat Transfer from Flames,* Int., J.Heat Mass Transfer, Vol.15, 1972, pp.2155-2172.

18. James R.Welty, *Engineering Heat Transfer,* John Wiley & Sons, 1974.

19. A. G. Gaydon and H.G.Wolfhard, *Flames, Their Structure, Radiation and Temperature,* 4th Edition, "A Halsted Press Book," John Wiley & Sons, 1979.

20. Charles Anderson, private communications.

21. D. Brian Spalding, *GENMIX: A General Computer Program for Two-Dimensional Parabolic Phenomena,* Pergamon Press, Elmsford, NY, 1977.

APPENDIX A

RECORDED DATA FROM TESTS

NOMENCLATURE

A: Liquid valve opening

B: Vapor valve opening

G: Orifice pressure * 3 (PSIG)

N: Thermogage calorimeter * 10 (BTU/ft^2-sec)

O: Hastings velocimeter * 0.5 (ft/min: air @ STP)

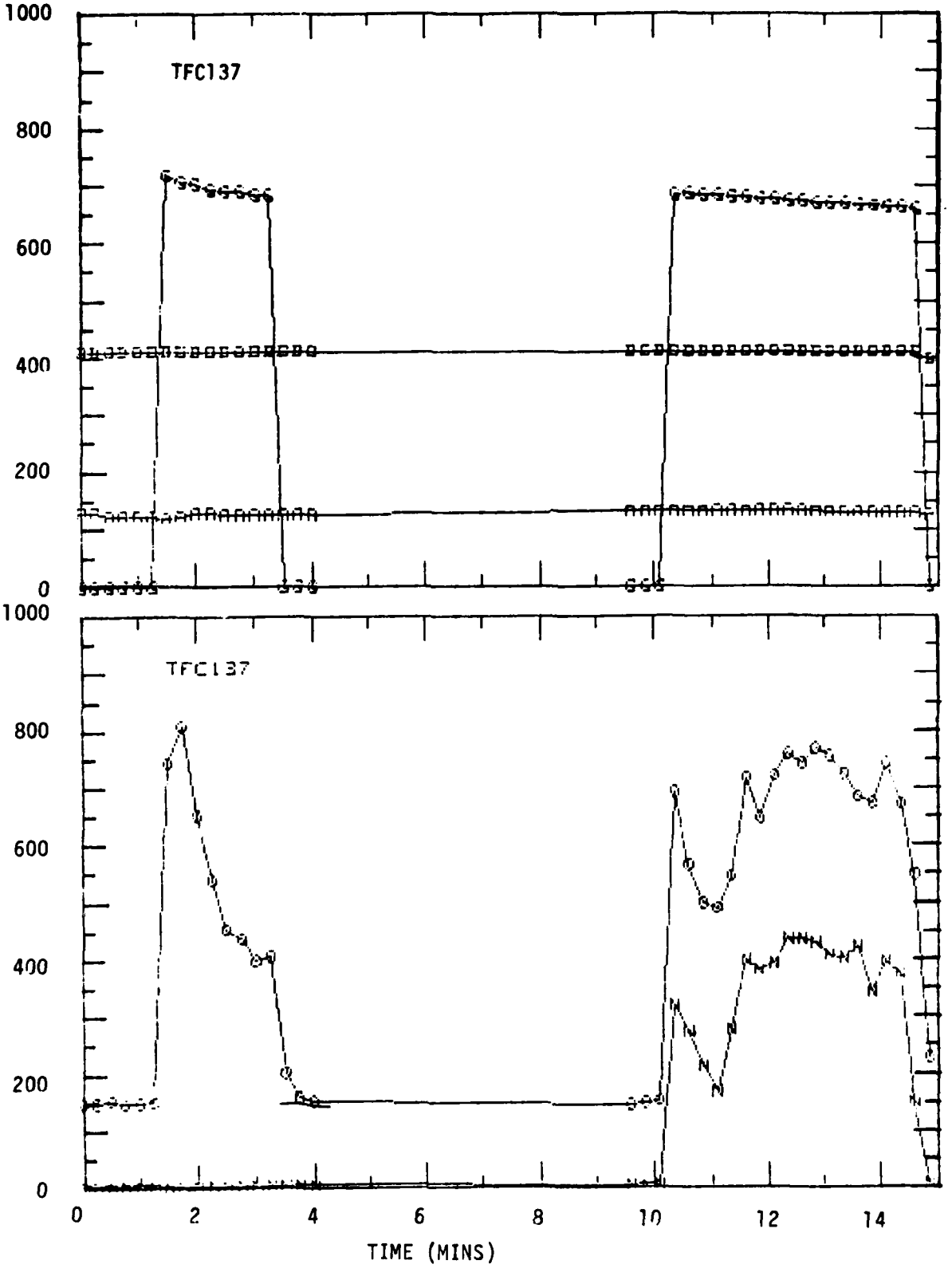
TFC137
1000
800
600
400
200
0
TFC137
1000
800
600
400
200
0
0
2
4
6
8
10
12
14
TIME (MINS)

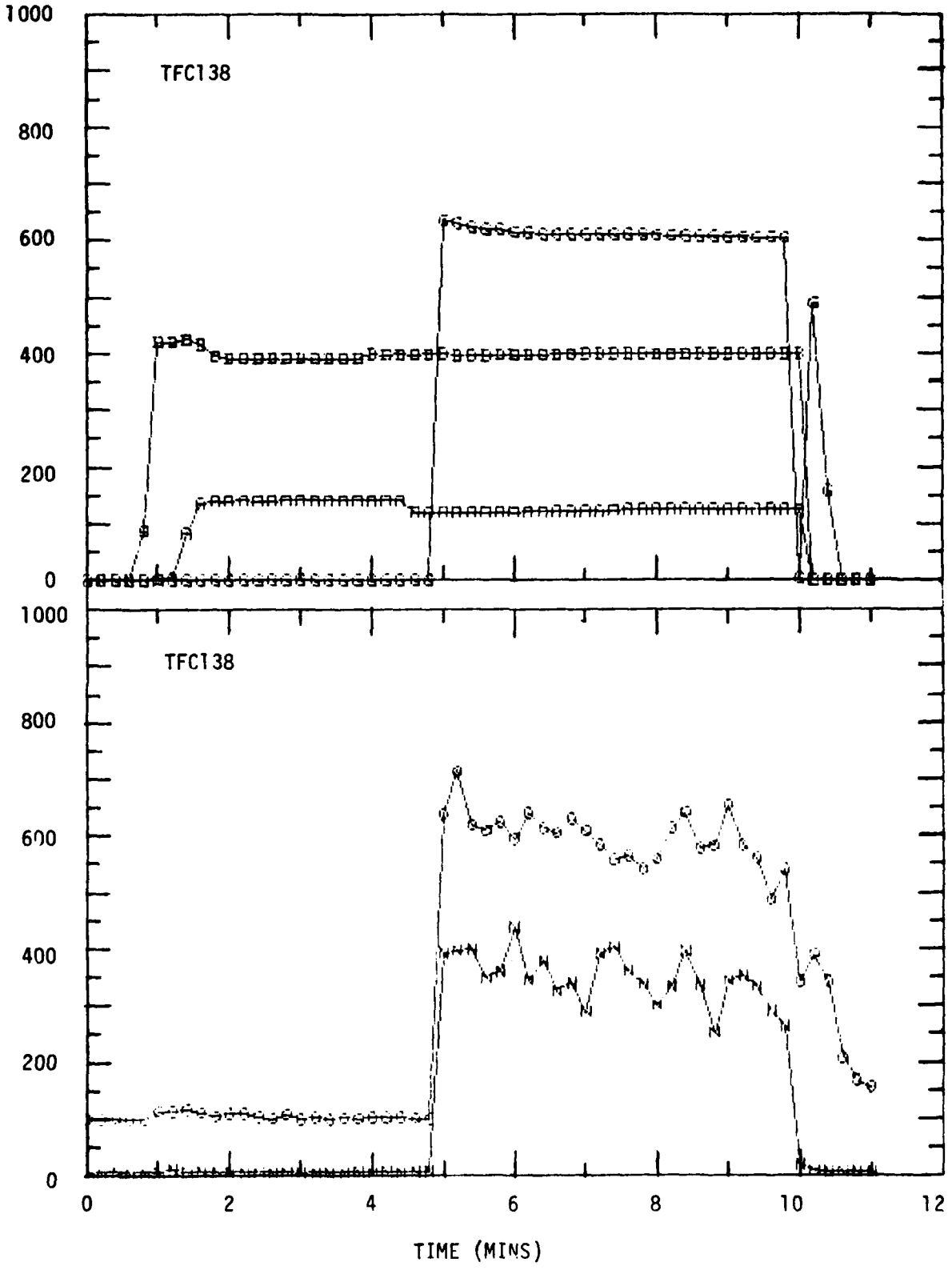
TFC138
1000
800
600
400
200
0
TFC138
1000
800
600
400
200
0
0
2
4
6
8
10
12
TIME (MINS)

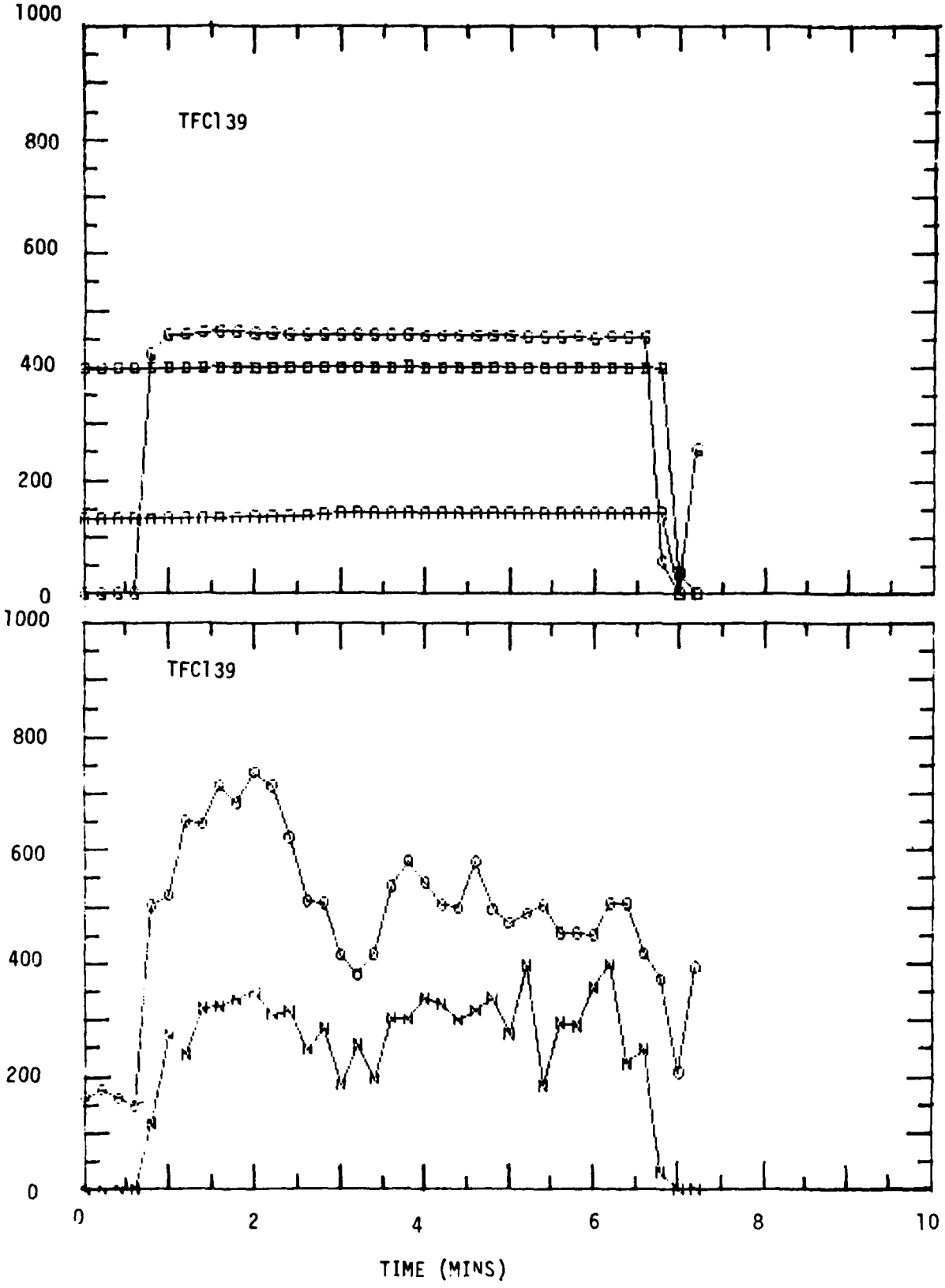
1000
800
600
400
200
0
TFC139
1000
800
600
400
200
0
TFC139
0
2
4
6
8
10
TIME (MINS)

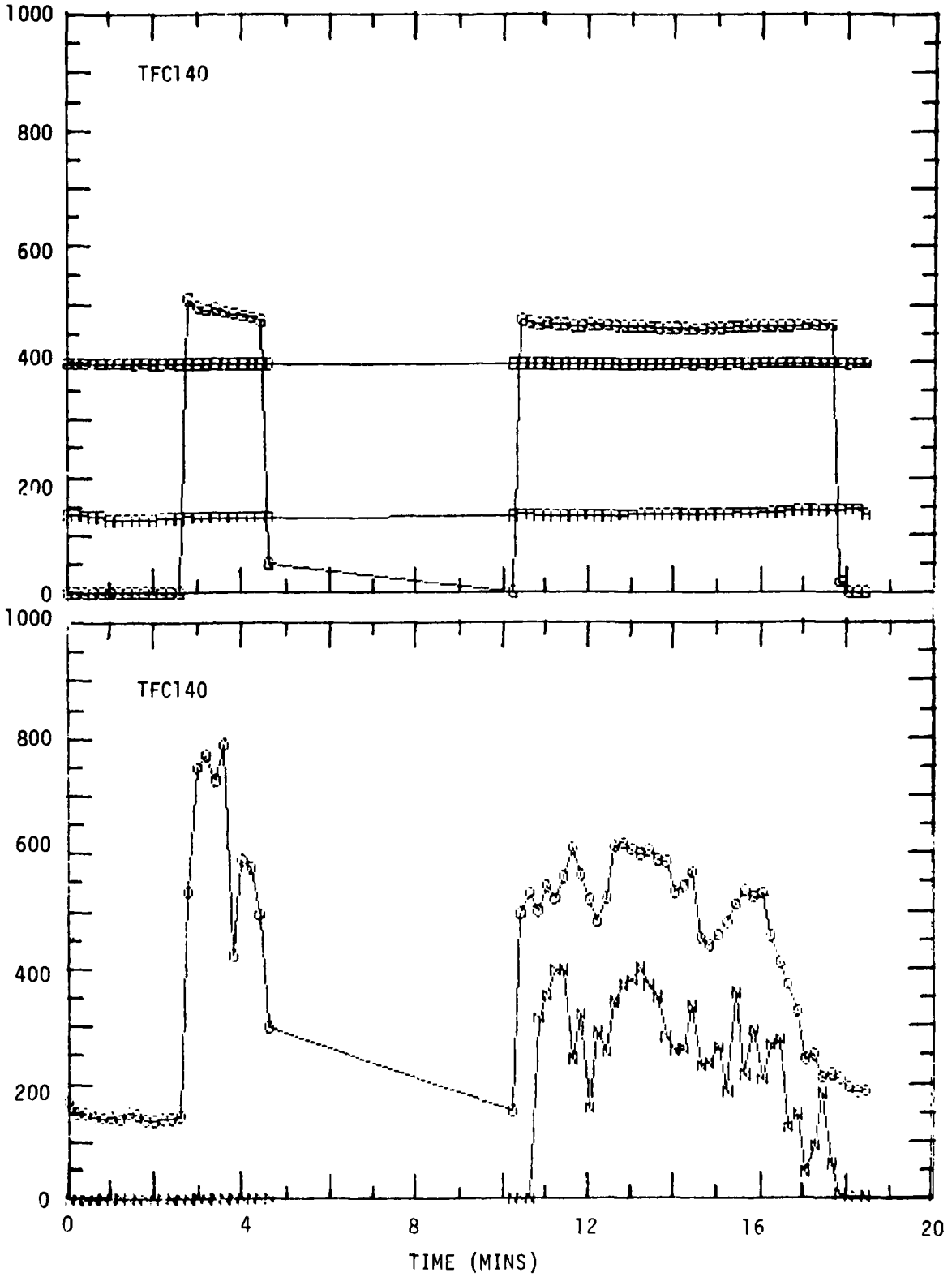
TFC140
1000
800
600
400
200
0
TFC140
1000
800
600
400
200
0
0
4
8
12
16
20
TIME (MINS)

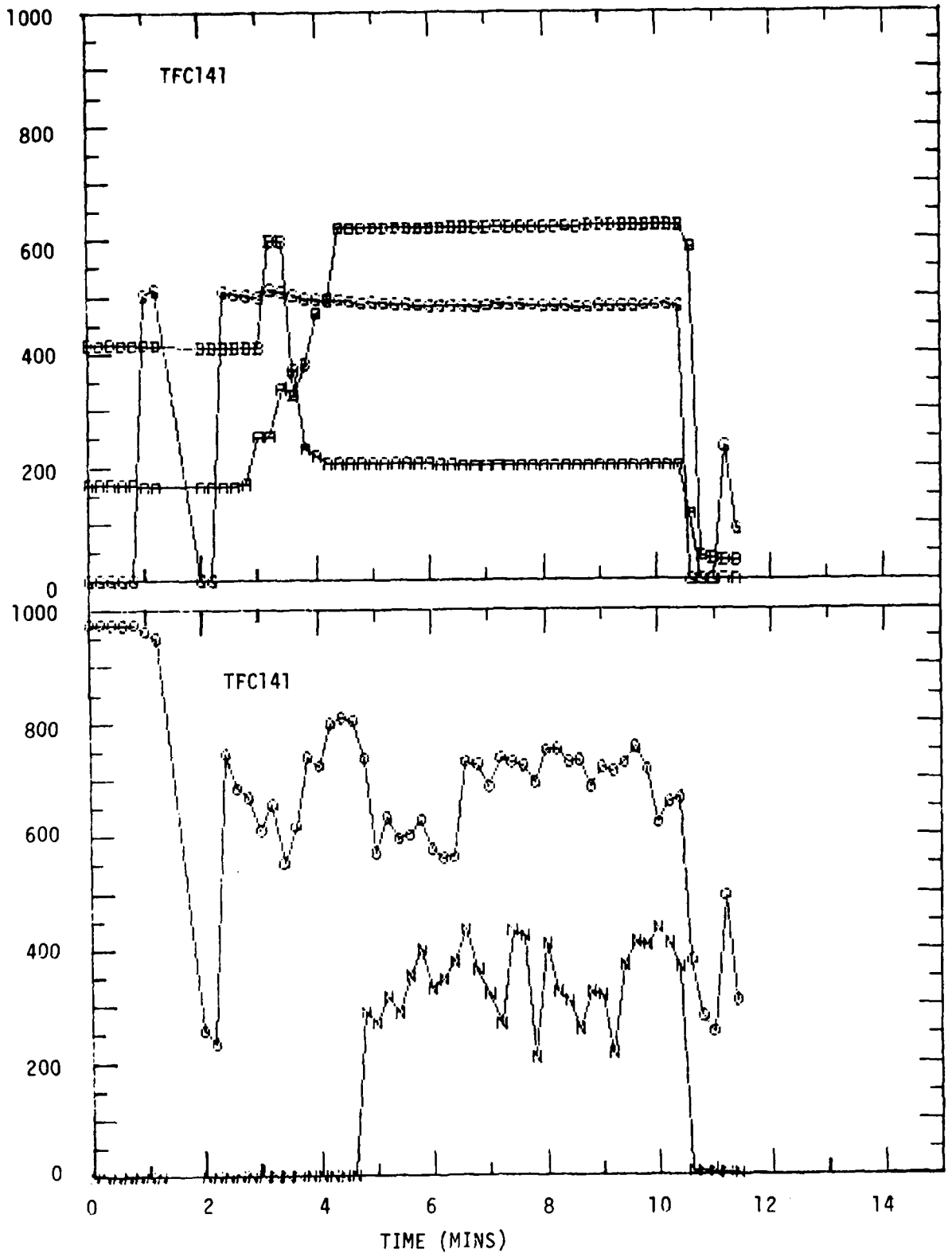
TFC141
1000
800
600
400
200
0
TFC141
1000
800
600
400
200
0
0
2
4
6
8
10
12
14
TIME (MINS)

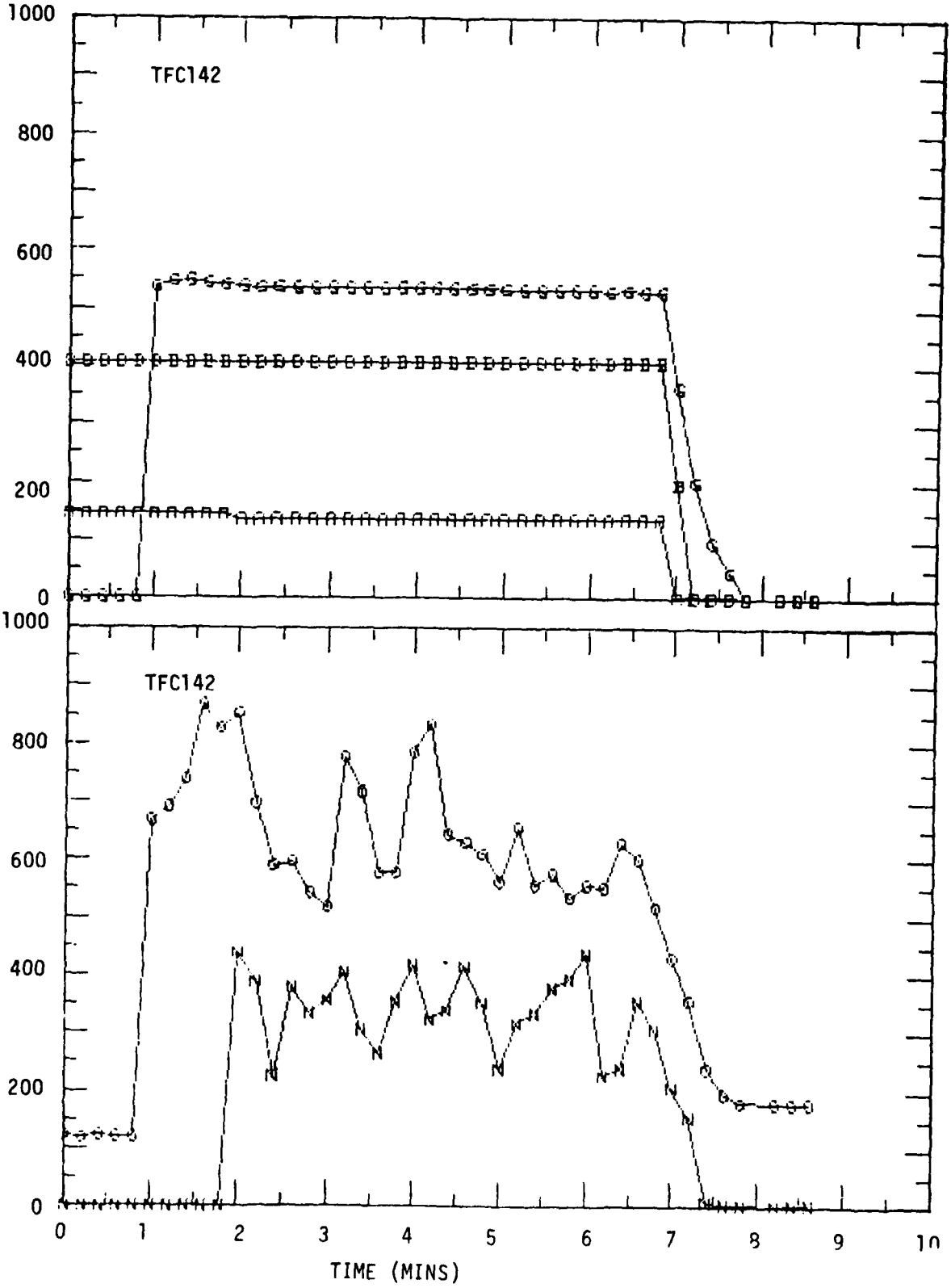
TFC142
1000
800
600
400
200
0
TFC142
1000
800
600
400
200
0
0
1
2
3
4
5
6
7
8
9
10
TIME (MINS)

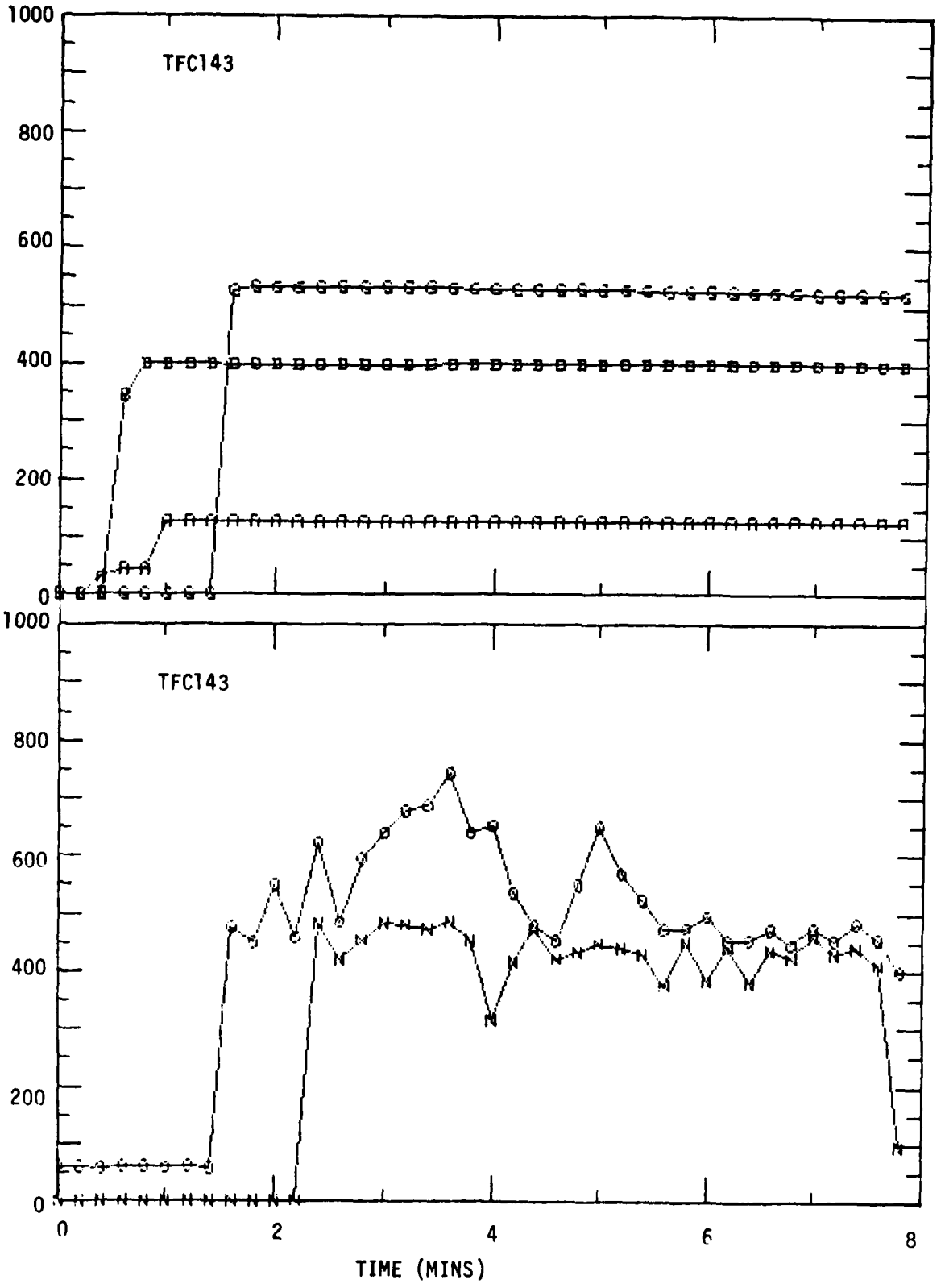
TFC143
1000
800
600
400
200
0
TFC143
1000
800
600
400
200
0
0
2
4
6
8
TIME (MINS)

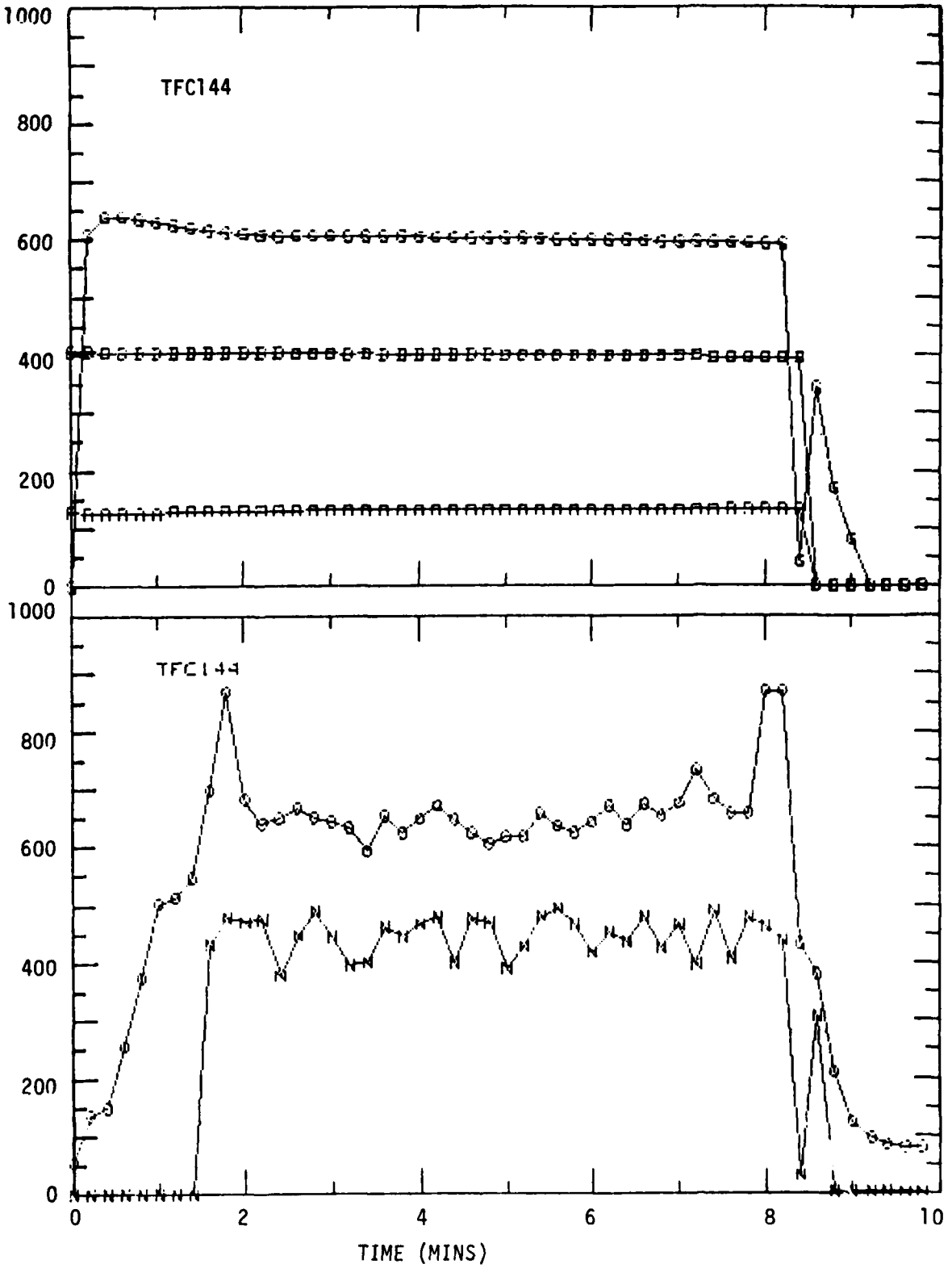
TFC144
1000
800
600
400
200
0
TFC144
1000
800
600
400
200
0
0
2
4
6
8
10
TIME (MINS)

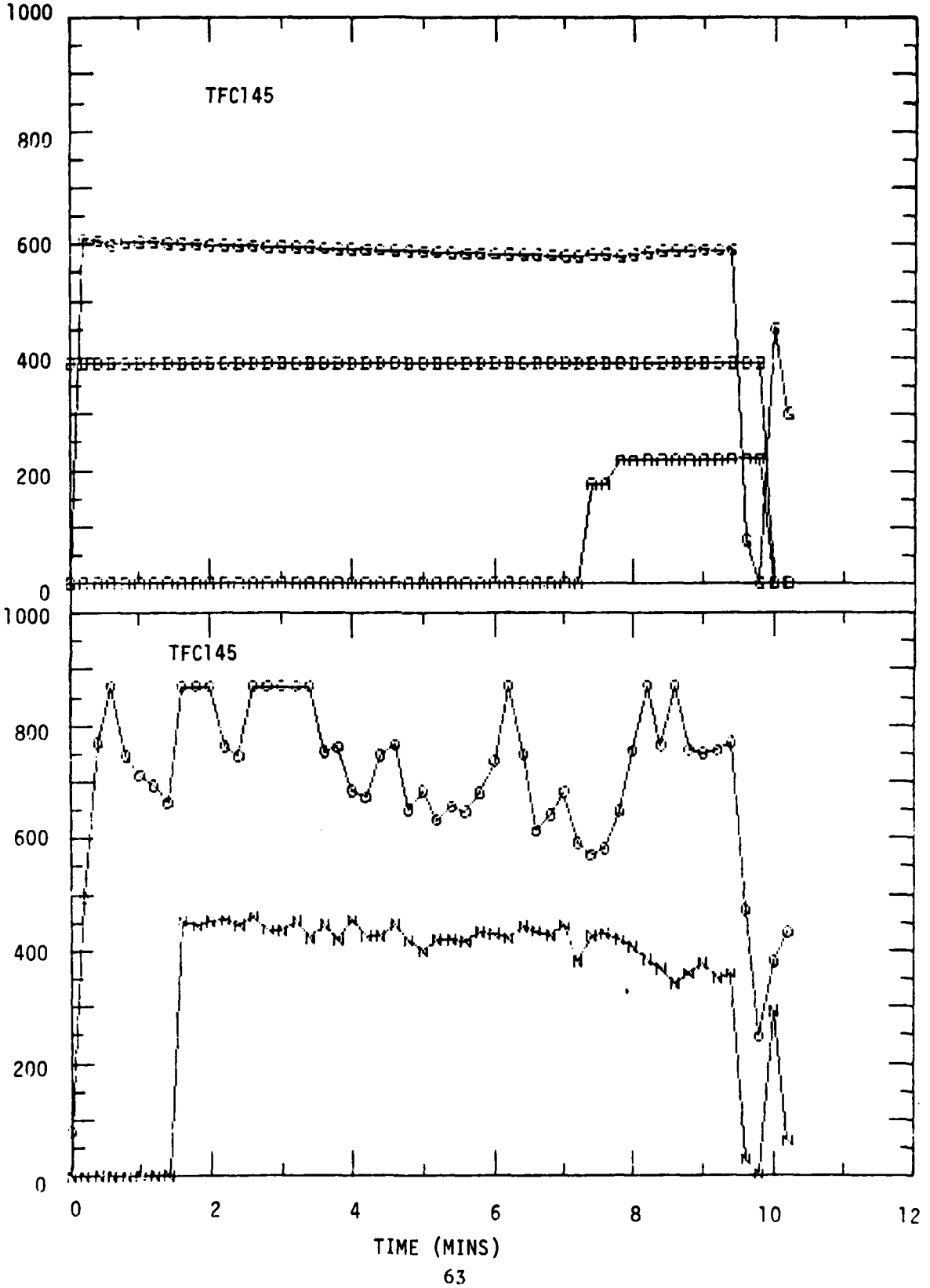
TFC145
1000
800
600
400
200
0
TFC145
1000
800
600
400
200
0
0
2
4
6
8
10
12
TIME (MINS)

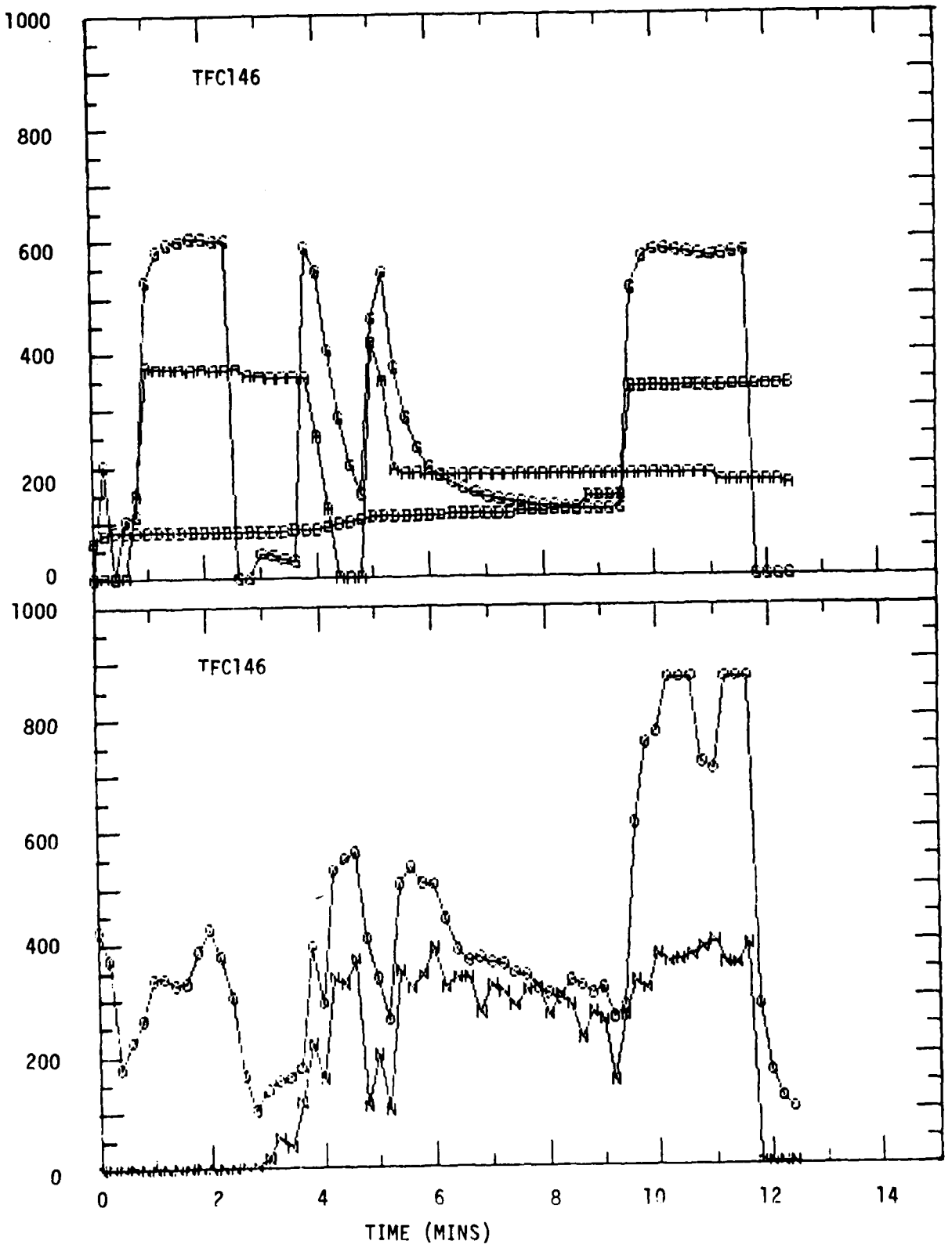
TFC146
1000
800
600
400
200
0
TFC146
1000
800
600
400
200
0
0
2
4
6
8
10
12
14
TIME (MINS)

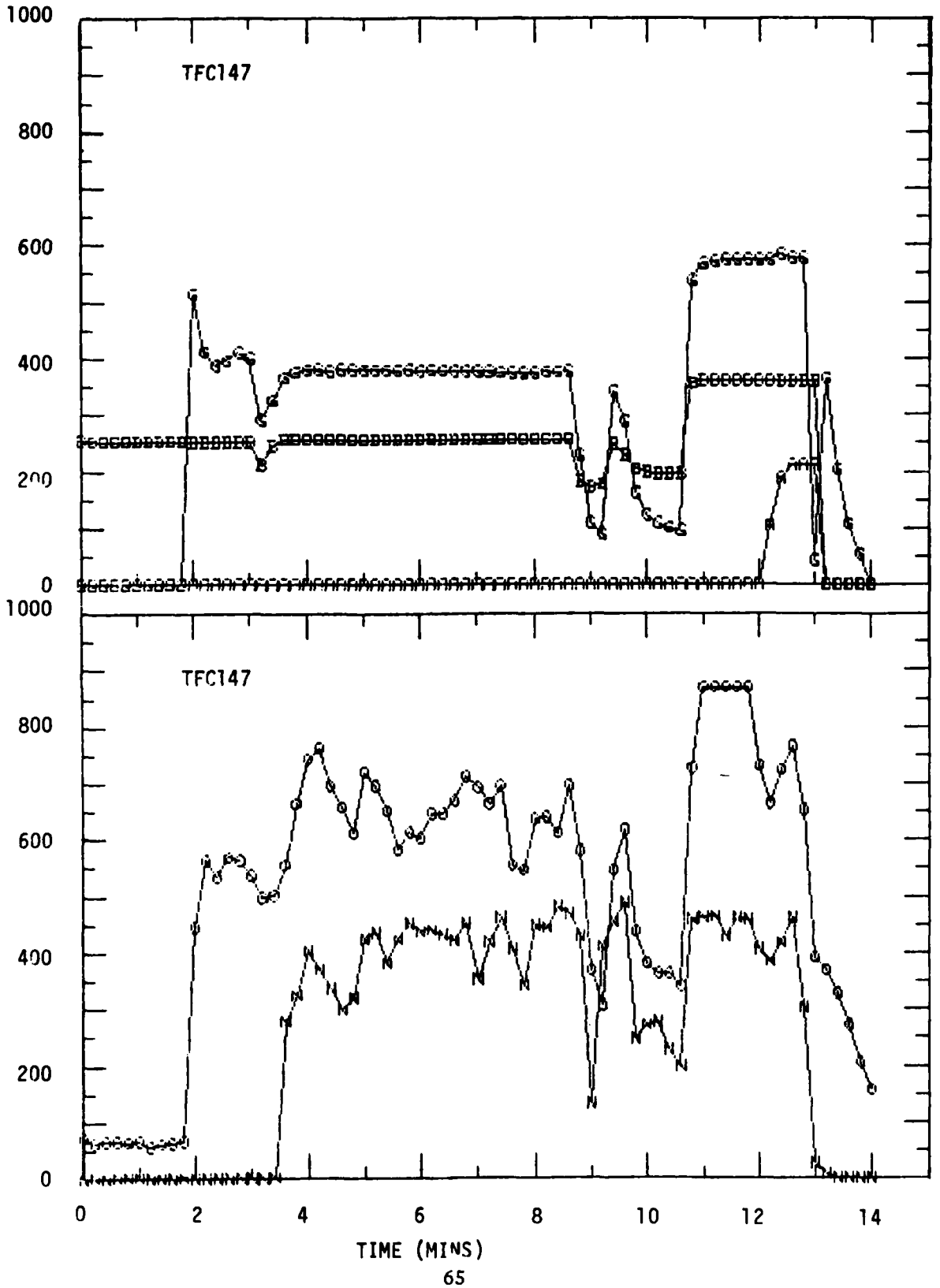
TFC147
1000
800
600
400
200
0
TFC147
1000
800
600
400
200
0
0
2
4
6
8
10
12
14
TIME (MINS)

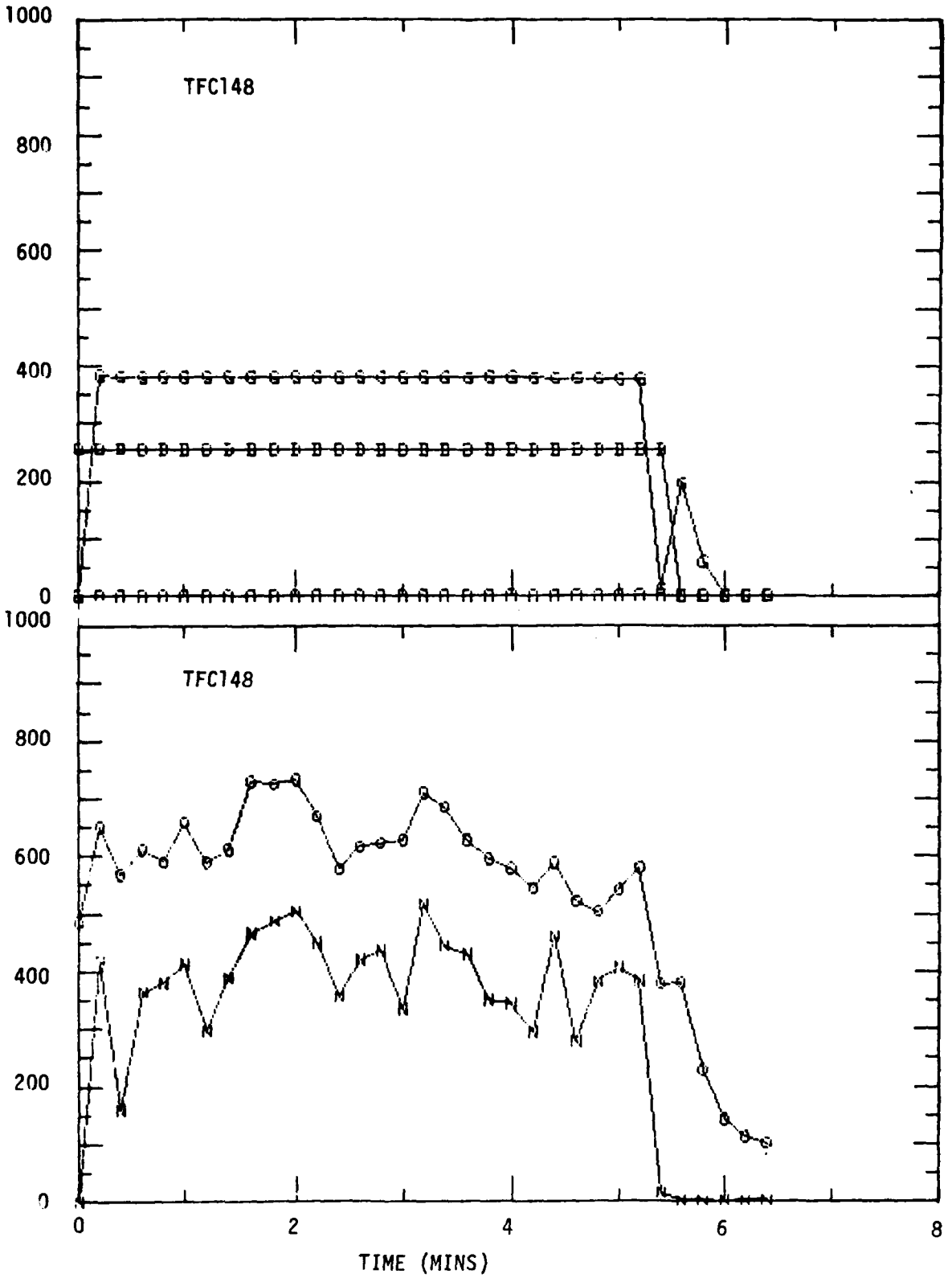
TFC148
1000
800
600
400
200
0
TFC148
1000
800
600
400
200
0
0
2
4
6
8
TIME (MINS)

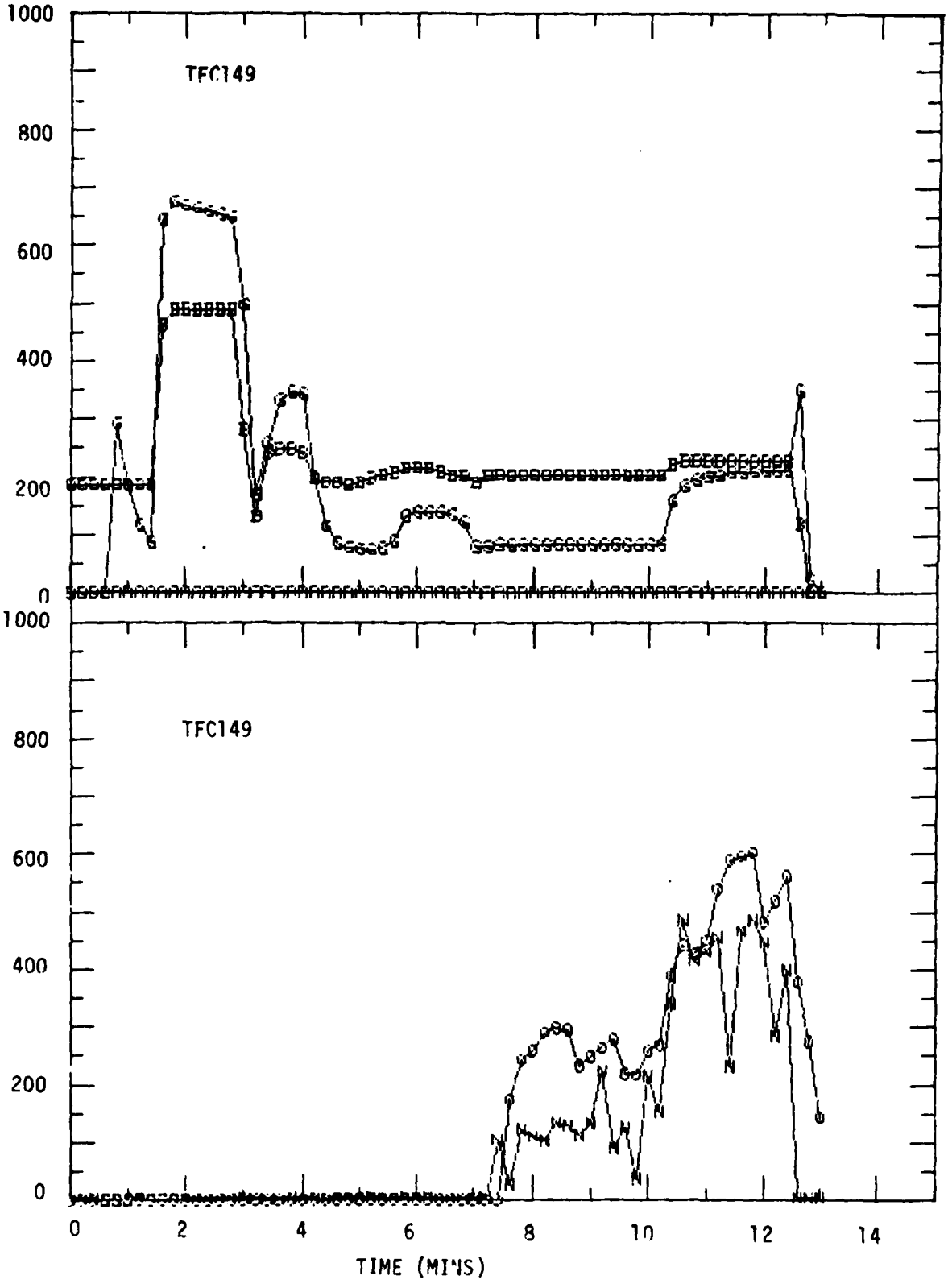
TFC149
1000
800
600
400
200
0
TFC149
1000
800
600
400
200
0
0
2
4
6
8
10
12
14
TIME (MINS)

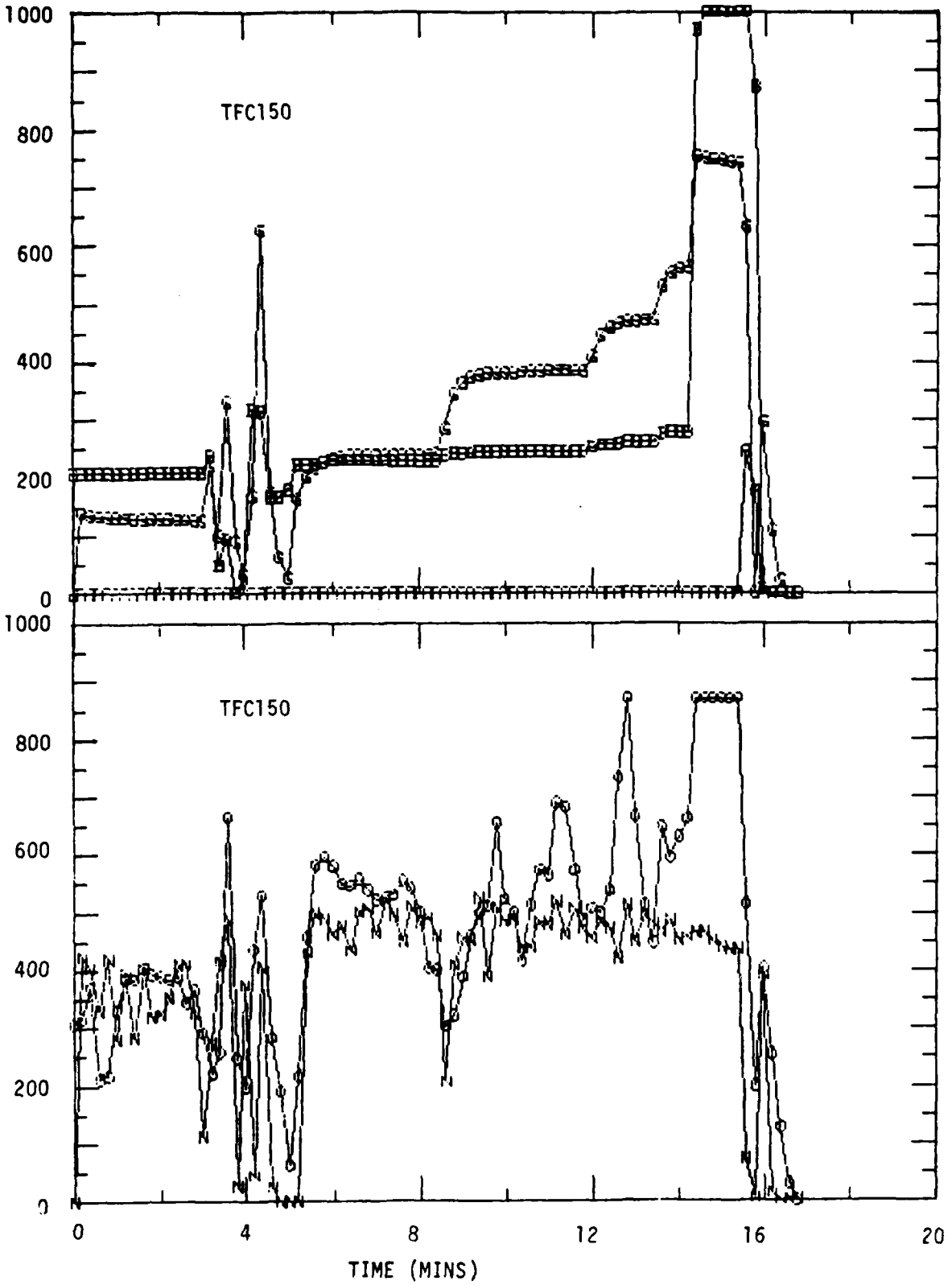
TFC150
TFC150
1000
800
600
400
200
0
0
4
8
12
16
20
TIME (MINS)

APPENDIX B

TABULATION CF COMPUTER MODEL

```
      PROGRAM HOTPLT
      DIMENSION TS(100,8),T(100,8,2),HTC(100,8)
      DIMENSION THEAD(125),HTCBAR(100,8)
      DIMENSION P(20),TK(20),SF(20),SG(20),HF(20),HG(20),VF(20),VG(20),
     +VEL(20),X(20),H(20),RHO(20),V(20),WDOTA(20),S(20)
      DIMENSION PPR(10),MOF(10),VASTPC(10,10),QC(10,10)
      COMMON/PRMTRS/TS,T,HTC,TRES,TA
      REAL MUBAR,KBAR,MUA,KI,KS,KSTL,MEFF,KAPPA,MW,MRATIO,MACHCP,MWCPC
      REAL IGDST,MOF
      DATA HTC,HTCBAR/1600*0.0/
      DATA T,TS,TINF/2401*549.1/
      OPEN (UNIT=1,NAME='HOTIN.DAT',TYPE='OLD')
      OPEN (UNIT=2,NAME='HOTOUT.DAT',TYPE='NEW')
      OPEN (UNIT=4,NAME='HOTLIP.DAT',TYPE='NEW')
C
C INPUT QUANTITIES AND DIMENSIONS
C   I    THSTL=PLATE THICKNESS (FT)
C   I    TA=TEMPERATURE OF JET TIP (R)
C   I    KI=THERMAL CONDUCTIVITY OF INSULATION (BTU/SEC-FT-F)
C   I    THI=INSULATION THICKNESS (FT)
C   I    KS=THERMAL CONDUCTIVITY OF SOOT (BTU/SEC-FT-F)
C   I    THS=SOOT THICKNESS (FT)
C   I    TINF=AMBIENT TEMPERATURE=INITIAL PLATE TEMPERATURE (R)
C   I    BETA=TILT ANGLE OF PLATE FROM HORIZONTAL (DEG)
C   I    PLDST=DISTANCE FROM NOZZLE TO PLATE (FT)
C        PBDST=DISTANCE FROM NOZZLE TO PROBE (FT)
C        IGDIST=DISTANCE FROM NOZZLE TO IGNITOR (FT)
C   I    Z=COMPRESSIBILITY OF PROPANE AT PEFF AND TA
C   I    RT=NOZZLE THROAT RADIUS (FT)
C   I    PLATE=HALF SPAN OF SMALLEST PLATE EDGE (FT)
C   I    DELT=TIME INCREMENT SELECTED, MUST BE LESS THAN DELT1 AND
C             DELT2 (SEC)
C   I    E=EMISSIVITY OF SURFACE MATERIAL
C
C   C    DELT1=LARGEST TIME INCREMENT ALLOWED TO COMPUTE T(I,J,L) FOR
C             THE CENTER ELEMENT (SEC)
C   C    DELT2=LARGEST TIME INCREMENT ALLOWED TO COMPUTE T(I,J,L) FOR
C             THE GENERAL ELEMENTS (SEC)
C   C    TRES=THERMAL RESISTANCE OF SOOT AND INSULATION (SEC-FT/BTU)
C   C    TS(I,J)=TEMPERATURE OF EACH ELEMENT OF THE FRONT SIDE OF PLATE (R)
C   C    T(J,I,L)=TEMPERATURE OF EACH ELEMENT OF THE PLATE BACK SIDE (R)
C   C    HTCBAR(I,J)=CONVECTIVE HEAT TRANSFER COEFF. AT BACK SURFACE
C            OF PLATE
C   C    HTC(I,J)=HEAT TRANSFER COEFFICIENT AT FRONT SURFACE MATERIAL
C   C    THT=ANGULAR DISTANCE FROM ZERO-DEGREE LINE TO ELEMENT CENTER
C            (DEG)
C   C    R=RADIAL DISTANCE FROM PLATE CENTER TO ELEMENT CENTER (FT)
C   C    DELR=RADIAL DIMENSION OF PLATE ELEMENTS, EQUALS RA
C   C    N=NUMBER OF RADIAL ELEMENTS USED
```

```
C    C     RAT=RADIUS OF JET AT THE PLATE (FT)
C    C     VA=JET VELOCITY AT THE PLATE (FPS)
C    C     REFF=EFFECTIVE RADIUS OF JET (FT)
C    C     DEFF=EFFECTIVE DENSITY OF JET (LB/CUBIC FT)
C    C     MEFF=JET MACH NO.
C    C     N=LIMIT ON NUMBER OF RADIAL ELEMENTS USED
C
C    A     I=RADIAL INDEX
C    A     J=ANGULAR INDEX
C    A     KSTL=THERMAL CONDUCTIVITY OF STEEL (BTU/SEC-FT-F)
C    A     DSTL=DENSITY OF STEEL (LB/CUBIC FT)
C    A     HC=SPECIFIC HEAT OF STEEL (BTU/LB-F)
C    A     DA=DENSITY OF COMBUSTION PRODUCTS AT 2500F (LB/CUBIC FT)
C    A     MUA=VISCOSITY OF COMBUSTION PRODUCTS AT 2500F (LB/FT-SEC)
C    A     MBAR=THERMAL CONDUCTIVITY OF COMBUSTION PRODUCTS AT 1500F
C               (BTU/SEC-FT-F)
C    A     MUBAR=VISCOSITY OF COMBUSTION PRODUCTS AT 1500F (LB/FT-SEC)
C    A     CPBAR=CONSTANT PRES. SPECIFIC HEAT OF COMB. PRODUCTS AT
C               1500F (BTU/LB-F)
C    A     M=NUMBER OF ANGULAR ELEMENTS USED
C    A     DELTHT=ANGULAR DIMENSION OF PLATE ELEMENTS
C    A     DAIR=DENSTIY OF AIR (LB/CUBIC FT)
C    A     PEFF=EFFECTIVE PRESSURE OF JET (PSIA)
C    A     RP=GAS CONSTANT FOR PROPANE (FT-LB/LBM-R)
C    A     GC=DIMENSIONAL CONSTANT (LBM-SEC SQ/LB-FT)
C    A     GAM=SPECIFIC HEATS RATIO OF PROPANE
C    A     SIGMA=STEFAN-BOLTZMANN CONSTANT (BTU/SEC-SQFT-R**4)
C      TEMP-ENTROPY DIAGRAM FOR PROPANE. P = ATM
C      TK = DEG K
C      SF,SG = CAL/(MOLE-K)
C      HF,HG = CAL/MOLE
C      VF,VG = CM3/MOLE
C      PR = RESERVOIR PRESSURE,PSIA
C      XR = RESERVOIR QUALITY, DIMENSIONLESS
C      MW = MOLECULAR WEIGHT OF PROPANE, GM/MOLE
C
C      TEFFK  = TEMP OF PROPANE AT P=1ATM, (K)
C      MWPC   = MOLECULAR WEIGHT OF PROPANE, (GM/MOLE)
C      VEFFC  = VELOCITY OF EXPANDED PROPANE AT 1 ATM, (CM/SEC)
C      ROEFFC = DENSITY OF EXPANDED PROPANE AT 1 ATM, (GM/CM**3)
C      AEFFC  = AREA OF EXPANDED PROPANE AT 1 ATM, (CM**2)
C      RAEFFC = RADIUS OF EXPANDED PROPANE AT 1 ATM, (CM)
C      HEFFC  = ENTHALPY OF EXPANDED PROPCANE AT 1 ATM, (ERG/GM)
C      UCPC   = INITIAL VELOCITY OF COMB. PROD., (CM/SEC)
C      HEJC   = TOTAL INTERNAL ENERGY OF EXPANDED PROPANE DEPOSITED TO
C               COMBUSTION PRODUCTS, (ERGS/GM)
C      TCPK   = INITIAL TEMPERATURE OF COMB. PROD., (K)
C      ROCPC  = INITIAL DENSITY OF COMB. PROD., (GM/CM**3)
C      HCPC   = ENTHALPY OF COMB. PROD., (ERGS/GM)
```

```
C      CPCPC  = CONSTANT PRESSURE SPECIFIC HEAT OF COMB. PROD.,
C               (ERG/(GM*K))
C      MWCPC  = MOLECULAR WEIGHT OF COMBUSTION PRODUCTS, (GM/MOLE)
C      AOCPC  = SPEED OF SOUND OF COMB. PROD., (CM/SEC)
C      MACHCP = INITIAL MACH NO OF COMB. PROD., (-)
C      ROAIRC = DENSITY OF AIR, (GM/CM**3)
C      ACPC   = INITIAL AREA OF COMBUSTION PRODUCTS, (CM**2)
C      RACPC  = INITIAL RADIUS OF COMB. PROD., (CM)
C      AC     = DISTANCE FROM INITIAL COMB. REGION TO PLATE, (CM)
C      VAC    = VELOCITY OF MIX AT PLATE, (CM/SEC)
C      RADAC  = RADIUS OF MIX AT PLATE, (CM)
C      HEQCPC = TOTAL INTERNAL ENERGY OF MIX AT PLATE, (ERG/GM)
C      HAC    = ENTHALPY OF MIX AT PLATE
C      TAK    = TEMPERATURE OF MIX AT PLATE, (K)
C
C
C       READ ALL INPUT DATA
C
     1 READ(1,1000,END=2000)
       READ (1,6) NNLOOP
       DO 8 I=1,NNLOOP
     8 READ (1,1010)PPR(I),MOF(I)
     5 READ(1,1010)XR,MW,RP
       DO 10 I=1,18
    10 READ(1,1010)P(I),TK(I),SF(I),SG(I),HF(I),HG(I),VF(I),VG(I)
C       READ FLAME DIMENSIONS
       READ (1,920)CD,RAT,TA
C       READ PLATE DIMENSIONS
       READ (1,930) PLDST,PBDST,IGDST,BETA,THSTL,PLATE
C       READ INSULATION DIMENSIONS
       READ (1,910)THI,KI
C       READ SOOT DIMENSIONS
       READ (1,910)THS,KS
C       READ PROPANE COMPRESSIBILITY, LIMIT OF ITERATIONS
       READ (1,940)Z,LIMIT
C       READ TIME INCREMENT
       READ (1,945)DELT
C       READ EMISSIVITY OF SURFACE MATERIAL
       READ (1,945)E
       READ (1,53)(THEAD(II),II=1,125)
       DO 9997 II=1,NNLOOP
       DO 9997 JJ=1,NNLOOP
C
C       DEFINE CONSTANTS FOR PROPANE PROBLEM
C
       GAM=1.15
       RCONC=8.31E7
       MRATIO=7.6928
       HAIRC=5.023E10
```

```
      TAIRK=298.15
      GC=32.17
      DAIR=0.0765
      DELTHT=0.5235987757
      MUA=3.5E-5
      DA=0.013
      KSTL=6.944E-3
      DSTL=490.
      HC=0.11
      CPBAR=0.313
      MUBAR=2.76E-5
      KBAR=1.16E-5
      SIGMA=4.76111E-13
      SIGMAC=5.67E-5
      EPSLNC=0.2
      PI=3.141592654
      UMAXC=1600.*12.*2.54
      RT=RAT*CD**.5
C
C       CALCULATE RESERVOIR CONDITIONS
C
      PR=PPR(II)/14.7
      MRATIO=MOF(JJ)+2.
      I=1
   15 IF(P(I)-PR)25,30,20
   20 I=I+1
      GO TO 15
   25 ISAVE=I
      PRATIO=(PR-P(I-1))/(P(I)-P(I-1))
      TR =TK(I-1)+(TK(I)-TK(I-1))*PRATIO
      SFR=SF(I-1)+(SF(I)-SF(I-1))*PRATIO
      SGR=SG(I-1)+(SG(I)-SG(I-1))*PRATIO
      HFR=HF(I-1)+(HF(I)-HF(I-1))*PRATIO
      HGR=HG(I-1)+(HG(I)-HG(I-1))*PRATIO
      VFR=VF(I-1)+(VF(I)-VF(I-1))*PRATIO
      VGR=VG(I-1)+(VG(I)-VG(I-1))*PRATIO
      SR=(1.-XR)*SFR+XR*SGR
      HR=(1.-XR)*HFR+XR*HGR
      VR=(1.-XR)*VFR+XR*VGR
      GO TO 35
   30 ISAVE=I
      SFR=SF(I)
      SGR=SG(I)
      HFR=HF(I)
      VFR=VF(I)
      VGR=VG(I)
      SR=(1.-XR)*SFR+XR*SGR
      HR=(1.-XR)*HFR+XR*HGR
      VR=(1.-XR)*VFR+XR*VGR
```

```
   35 WRITE(2,1000)
      WRITE(2,1025)PR,XR,TR,SFR,SGR,SR,HFR,HGR,HR,VFR,VGR,VR
C
C     ISENTROPIC EXPANSION FROM RESERVOIR CONDITIONS TO CHOKED FLOW
C     AT NOZZLE THROAT
C
      WRITE(2,1028)
      J=ISAVE
      K=1
   40 X(J)=(SR-SF(J))/(SG(J)-SF(J))
      V(J)=(1.-X(J))*VF(J)+X(J)*VG(J)
      H(J)=(1.-X(J))*HF(J)+X(J)*HG(J)
      S(J)=SR
      RHO(J)=MW/V(J)
      VEL(J)=SQRT(2.*(HR-H(J))*4.186E7/MW)
      WDOTA(J)=RHO(J)*VEL(J)
      WRITE(2,1030)X(J),V(J),H(J),S(J),RHO(J),VEL(J),WDOTA(J),P(J)
      IF(K.EQ.2)GOTO 45
      J=J+1
      K=2
      GOTO 40
   45 IF (WDOTA(J)-WDOTA(J-1))55,55,50
   50 J=J+1
      GOTO 40
C
C     CURVE FIT FOR PT AT WDOTA MAX
C     FIT PARABOLA THROUGH J,J-1 AND J-2
C
   55 ENUM=(WDOTA(J)-WDOTA(J-1))*(P(J)-P(J-2))-(WDOTA(J)-WDOTA(J-2))
     +*(P(J)-P(J-1))
      DENOM=(P(J)**2-P(J-1)**2)*(P(J)-P(J-2))-(P(J)**2-P(J-2)**2)
     +*(P(J)-P(J-1))
      AA=ENUM/DENOM
      B=((WDOTA(J)-WDOTA(J-1))-AA*(P(J)**2-P(J-1)**2))/(P(J)-P(J-1))
      PT=-B/(2.*AA)
C
C     INTERPOLATION FOR THROAT CONDITIONS WHEN WDOTA IS MAXIMUM
C
      WRITE (2,1021) RAT,CD,RT
      RATIO=(PT-P(J-1))/(P(J)-P(J-1))
      TT =TK(J-1)+(TK(J)-TK(J-1))*RATIO
      SFT=SF(J-1)+(SF(J)-SF(J-1))*RATIO
      SGT=SG(J-1)+(SG(J)-SG(J-1))*RATIO
      HFT=HF(J-1)+(HF(J)-HF(J-1))*RATIO
      HGT=HG(J-1)+(HG(J)-HG(J-1))*RATIO
      VFT=VF(J-1)+(VF(J)-VF(J-1))*RATIO
      VGT=VG(J-1)+(VG(J)-VG(J-1))*RATIO
      XT=(SR-SFT)/(SGT-SFT)
      VT=(1.-XT)*VFT+XT*VGT
```

```
      HT=(1.-XT)*HFT+XT*HGT
      RHOT=MW/VT
      VELT=SQRT(2.*(HR-HT)*4.186E7/MW)
      WDOTAM=RHOT*VELT
      WDOTM=WDOTAM*PI*(RT*12.*2.54)**2
      WRITE(2,1035)PT,XT,TT,SFT,SGT,SR,HFT,HGT,HT,VFT,VGT,VT,RHOT,VELT,
     +WDOTAM,WDOTM
C
C   ISENTROPIC EXPANSION OF PROPANE FROM NOZZLE TO ATMOSPHERIC PRESSURE
C
      PEFF=1.0
      I=1
   60 IF(P(I).EQ.PEFF)GOTO 65
      I=I+1
      GOTO 60
   65 ISAVE=I
      TEFFK=TK(I)
      XEFF=(SR-SF(ISAVE))/(SG(ISAVE)-SF(ISAVE))
      SPVOL=(1.-XEFF)*VF(ISAVE)+XEFF*VG(ISAVE)
      ENTH=(1.-XEFF)*HF(ISAVE)+XEFF*HG(ISAVE)
      DENS=MW/SPVOL
      FLUX=DENS*SQRT(2.*(HR-ENTH)*4.186E7/MW)
      AEFF=WDOTM/FLUX
      REFF=SQRT(AEFF/PI)/(2.54*12.)
      VEFF=(FLUX/DENS)/(2.54*12.)
      TEFF=TA
C
C   NUMERICAL DIFFERENTIATION OF T-S DIAGRAM FOR PROPANE AT S=SR AND PEFF
C   TO OBTAIN SPEED OF SOUND
C
      P1=PEFF+0.1
      I=1
   70 IF(P(I).LT.P1)GOTO 75
      I=I+1
      GOTO 70
   75 RATIO=(P1-P(I-1))/(P(I)-P(I-1))
      SF1=SF(I-1)+(SF(I)-SF(I-1))*RATIO
      SG1=SG(I-1)+(SG(I)-SG(I-1))*RATIO
      X1=(SR-SF1)/(SG1-SF1)
      VF1=VF(I-1)+(VF(I)-VF(I-1))*RATIO
      VG1=VG(I-1)+(VG(I)-VG(I-1))*RATIO
      V1=(1.-X1)*VF1+X1*VG1
      RHO1=MW/V1
      P2=PEFF-0.1
      I=1
   80 IF(P(I).LT.P2)GOTO 85
      I=I+1
      GOTO 80
   85 RATIO=(P2-P(I-1))/(P(I)-P(I-1))
```

```
      SF2=SF(I-1)+(SF(I)-SF(I-1))*RATIO
      SG2=SG(I-1)+(SG(I)-SG(I-1))*RATIO
      X2=(SR-SF2)/(SG2-SF2)
      VF2=VF(I-1)+(VF(I)-VF(I-1))*RATIO
      VG2=VG(I-1)+(VG(I)-VG(I-1))*RATIO
      V2=(1.-X2)*VF2+X2*VG2
      RHO2=MW/V2
      DRHODP=ABS(RHO2-RHO1)/(2.*0.1)
      SONIC=SQRT((14.7*454.*980./(2.54**2))/DRHODP)/(12.*2.54)
      MEFF=VEFF/SONIC
      RHOEFF=144.*14.7*PEFF/(Z*RP*TEFF)
      PEFF=14.7
      PEFFC=PEFF*6.895E4
      DEFF=RHOEFF
      WRITE(2,1040)REFF,VEFF,TEFF,SONIC,MEFF,RHOEFF,PEFF
      MWPC=MW
      VEFFC=VEFF*2.54*12.
      ROEFFC=PEFFC*MWPC/(RCONC*TEFFK)
      AEFFC=AEFF
      RAEFFC=REFF*2.54*12
      HEFFC=ENTH*(1/MWPC)*4.186E7
      WRITE(2,1045)PEFFC,VEFFC,ROEFFC,AEFFC,RAEFFC,HEFFC,TEFFK
C
C  END OF EXPANSION TO ATM CONDITIONS
C
C  BEGIN COMBUSTION
C
      UMIXC=(1.+MRATIO))*VEFFC
C     HEQC=HEFFC+((VEFFC**2.-UCPC**2.)/2.)
      TUOXOK=133.9*MRATIO+337.3
      DTDXMK=-2.4734*MRATIO+50.73
      DTDUMK=-0.6878*MRATIO+14.091
      TUOXXK=TUOXOK+DTDXMK*XEFF
      TCPK=(UMIXC/UMAXC)*DTDUMK+TUOXXK
      MWCPC=0.7456*MRATIO+17.44
      HNOT=34786.0/MWCPC
      DHDXM=-0.99*MRATIO+19.42
      HXOM=7.0*MRATIO-129.7
      HCP=HXOM+DHDXM*XEFF
      HCPC=(HCP+HNOT)*4.186E7
      ROCPC=(PEFFC*MWCPC)/(RCONC*TCPK)
      GAMCPC=-8.254E-3*MRATIO+1.3635
      UCPC=UMIXC
      AOCPC=(GAMCPC*RCONC*TCPK/MWCPC)**0.5
      CPCPC=1.538E7
      MACHCP=UCPC/AOCPC
      WRITE(2,1055)TUOXOK,DTDXMK,DTDUMK,TUOXXK,TCPK
      WRITE(2,1056)HNOT,DHDXM,HXOM,HCP,HCPC
      WRITE(2,1057)ROCPC,GAMCPC,UCPC,AOCPC,CPCPC
```

```
      ROAIRC=DAIR*1.605E-2
      ACPC=(ROEFFC*AEFFC*VEFFC)*(1.+MRATIO)/(ROCPC*UCPC)
      RACPC=SQRT(ACPC/PI)
      WRITE(2,1065)ROAIRC,ACPC,RACPC
      A=(PBDST-IGDST)
      AC=A*12.*2.54
      IF(MACHCP.LT.1.0)GOTO 90
      KAPPA=0.063*(MACHCP**2.-1)**(-0.15)
      GOTO 95
   90 KAPPA=0.08*(1.-0.16*MACHCP)*(ROAIRC/ROCPC)**(-0.22)
   95 DENOM=(KAPPA*(AC/RACPC)*(ROAIRC/ROCPC)**0.5)-0.7
      DENOM1=(((DENOM+.7)/KAPPA)*.102)-.7
      WRITE(2,1060)AC,KAPPA,DENOM
      VAC=UCPC*(1.-EXP(-1./DENOM))
      VA=VAC/(2.54*12)
      RADAC=(AC*0.07)-0.70*RACPC*(ROAIRC/ROCPC)**(-0.50)
      RA=RADAC/(2.54*12)
      HEQCPC=HCPC+(UCPC**2.)/2.-HAIRC
      HAC=HAIRC-(VAC**2.)/2.+HEQCPC*(1.-EXP(-1/DENOM1))
      TAK=TCPK+(HAC-HCPC)/CPCPC
      PO=PR
      TO=TR
      DO=MW/VR
      WRITE(2,62)PO,TO,DO,RT,TA,A,BETA,THSTL,PLATE
      WRITE(2,63)THI,KI,THS,KS,Z,LIMIT,E
      WRITE(2,965)PEFF,TEFF,MEFF,DEFF,AEFF,REFF,VEFF,VA,RA
      WRITE(2,1067)VAC,RADAC,HEQCPC,HAC,TAK
      ZOUTC=(PLDST-PBDST)*2.54*12.0
      UZWPC=VAC*(1-EXP(-2*(ZOUTC/RACPC)**2.))
      WRITE(2,1022) ZOUTC,UZWPC
      VASTPC(II,JJ)=UZWPC*(1.+(ROCPC/ROAIRC-1.)*UZWPC/UCPC)**.5
      DELR=RA
      N=PLATE/DELR+0.5
      IF (N.GT.3)GOTO 301
      N=4
      DELR=PLATE/(N-0.5)
  301 WRITE(2,52)DELR,N
C
C     CALCULATE HEAT TRANSFER COEFICIENTS AT FRONT SURFACE OF PLATE
C
      M=7
  205 BETA=BETA*PI/180.0
      RCEN=.2*DELR
      HTC(1,1)=(0.040*KBAR/RCEN)*(CPBAR*MUBAR/KBAR)**0.4
     +*(DA*VA*RCEN/MUA)**0.9
      HTCC=HTC(1,1)*2.044E7
C
C     300 DEG K IS THE ASSUMED WATER TEMPERATURE OF WATER IN THE PROBE
C
```

```
      QC(II,JJ)=HTCC*(TAK-300.)+SIGMAC*EPSLNC*(TAK**4-300.**4.)
      I=1
      WRITE(2,49)
      WRITE(2,48)
      DO 206 J=1,7
  206 HTC(1,J)=HTC(1,1)
      WRITE(2,950)(HTC(1,J),J=1,M),I
      DO 220 I=2,N
      RCEN=(I-1)*DELR
      DO 210 J=1,M
      THTCEN=DELTHT*(J+2)
      IF(J-4)207,208,209
  207 HTC(I,J)=0.040*(KBAR/RCEN)*(CPBAR*MUBAR/KBAR)**0.4*
     +((DA*VA*RCEN/MUA)*(1.0+COS(BETA))*(1+COS(BETA)*SIN(THTCEN)))**0.9
      GOTO 210
  208 HTC(I,J)=0.040*(KBAR/RCEN)*(CPBAR*MUBAR/KBAR)**0.4*
     +((DA*VA*RCEN/MUA))**0.9
      GOTO 210
  209 HTC(I,J)=0.040*(KBAR/RCEN)*(CPBAR*MUBAR/KBAR)**0.4*
     +((DA*VA*RCEN/MUA)*(1.0-COS(BETA))*(1+COS(BETA)*SIN(THTCEN)))**0.9
  210 CONTINUE
      WRITE(2,950)(HTC(I,J),J=1,M),I
  220 CONTINUE
      WRITE(2,7)
 9997 CONTINUE
      DO 9996 I=1,NNLOOP
      DO 9996 J=1,NNLOOP
      WRITE(4,3001)VASTPC(I,J)
 9996 WRITE(4,3001)QC(I,J)
      GOTO 2000
    6 FORMAT (I10)
 3001 FORMAT (E10.4)
    7 FORMAT (1H1)
  910 FORMAT (2F20.5)
  920 FORMAT (3F20.5)
  930 FORMAT (6F10.5)
  940 FORMAT (F20.5,I3)
  945 FORMAT (F10.4)
   48 FORMAT (8X,'90 DEG ',8X,'120 DEG ',7X,'150 DEG ',7X,'180 DEG ',7X,
     +'210 DEG ',7X,'240 DEG ',7X,'270 DEG ',8X,'R',//)
   49 FORMAT (1H1,40X,'HTC MATRIX (BTU/SEC-SQFT-F)',//)
  950 FORMAT (7F15.7,5X,I3,' DELR',/)
   52 FORMAT ('0DELR =',F14.6,12X,' N =',I4,/)
   53 FORMAT (80A1,/,45A1)
   62 FORMAT ('1PO =',E16.4,10X,'TO =',E16.4,10X,'DO =',E16.4,10X,'RJ ='
     +,E16.4,//,' TA=',E16.4,10X,'A =',E16.4,10X,'BETA =',E16.4,10X,'THS
     +TL =',E16.4,//,' PLATE =',E16.4,//)
   63 FORMAT ('0THI =',E16.4,10X,'KI =',E16.4,10X,'THS =',E16.4,10X,'KS
     +=',E16.4,//,' Z=',E16.4,10X,'LIMIT =',I10,10X,'E =',F5.3,//)
```

```
 965 FORMAT (6H PEFF=,E16.4,/,6H TEFF=,E16.4,/,6H MEFF=,16.4,/,6H DEFF=
    +,E16.4,/,6H AEFF=,E16.4,/,6H REFF=,E16.4,/,6H VEFF=,E16.4,/,4H VA=
    +,E16.4,/,4H RA=,E16.4,//)
  87 FORMAT ('0DELT =',E12.4,10X,'DELT1 =',E12.4,10X,'DELT2 =',E12.4,10
    +X,'TRES =',E12.4)
 350 FORMAT ('0+++++ TIME INCREMENT CHOSEN IS TOO LARGE, MUST BE LESS T
    +HAN OR EQUAL TO',E16.4,' SECONDS+++++')
 487 FORMAT (1H1,125A1,/)
 489 FORMAT ('    ')
 850 FORMAT(1H ,F14.2,F14.3,8X,'CENTER',E20.4,F16.2,F17.2)
 900 FORMAT (1H ,F14.2,F14.3,F14.1,E20.4,F16.2,F17.2)
 985 FORMAT (1X,99('+'),//)
1000 FORMAT (80H1
    +                                )
1010 FORMAT(6E12.6)
1025 FORMAT(1HO,11X,20HRESERVOIR CONDITIONS/
    +    2X,7HPR(ATM),22X,E9.3/
    +    2X,11HXR(QUALITY),18X,E10.4/
    +    2X,5HTR(K),24X,E11.5/
    +    2X,15HSFR(CAL/MOLE-K),14X,E10.4/
    +    2X,15HSGR(CAL/MOLE-K),14X,E10.4/
    +    2X,15HSR.(CAL/MOLE-K),14X,E10.4/
    +    2X,13HHFR(CAL/MOLE),16X,E10.4/
    +    2X,13HHGR(CAL/MOLE),16X,E10.4/
    +    2X,13HHR (CAL/MOLE),16X,E10.4/
    +    2X,13HVFR(CM3/MOLE),16X,E10.4/
    +    2X,13HVGR(CM3/MOLE),16X,E10.4/
    +    2X,13HVR (CM3/MOLE),16X,E10.4)
1021 FORMAT (1HO,2X,23HRADIUS OF THROAT (FEET),9X,E10.4/
    +            2X,6HCD (-),28X,E10.4/
    +            2X,30HEFFECTIVE THROAT RADIUS (FEET),2X,E10.4)
1028 FORMAT(1HO,10X,32HSEARCH FOR CHOKED FLOW AT THROAT/
    +  5X,1HX,5X,8HV(CM3/M),2X,8HH(CAL/M),2X,8HS(C/M-K),2X,9HRHO(G/CC),
    +  1X,8HVEL(C/S),4X,4HFLUX,6X,6HP(ATM))
1030 FORMAT(F8.4,3X,F8.1,3X,F7.1,3X,F6.2,3X,F8.5,2X,F8.1,2X,F7.2,4X,
    +F5.1)
1035 FORMAT(1HO,11X,17HTHROAT CONDITIONS/
    +    2X,7HPT(ATM),22X,E9.3/
    +    2X,11HXT(QUALITY),18X,E10.4/
    +    2X,5HTT(K),24X,E11.5/
    +    2X,15HSFT(CAL/MOLE-K),14X,E10.4/
    +    2X,15HSGT(CAL/MOLE-K),14X,E10.4/
    +    2X,15HST (CAL/MOLE-K),14X,E10.4/
    +    2X,13HHFT(CAL/MOLE),16X,E10.4/
    +    2X,13HHGT(CAL/MOLE),16X,E10.4/
    +    2X,13HHT (CAL/MOLE),16X,E10.4/
    +    2X,13HVFT(CM3/MOLE),16X,E10.4/
    +    2X,13HVGT(CM3/MOLE),16X,E10.4/
    +    2X,13HVT (CM3/MOLE),16X,E10.4/
```

```
     +    2X,12HRHOT(GM/CM3),17X,E10.4/
     +    2X,12HVELT(CM/SEC),17X,E10.4/
     +    2X,17HFLUXT(GM/CM2-SEC),2X,E10.4/
     +    2X,13HFLOWT(GM/SEC),4X,E10.4)
1040 FORMAT(1HO,7X,20HEFFECTIVE CONDITIONS/
     +    2X,8HREFF(FT),12X,E10.4/
     +    2X,9HVEFF(FPS),11X,E10.4/
     +    2X,7HTEFF(R),13X,E10.4/
     +    2X,10HSONIC(FPS),10X,E10.4/
     +    2X,4HMEFF,16X,E10.4/
     +    2X,14HRHOEFF(LB/FT3),6X,E10.4/
     +    2X,10HPEFF(PSIA),10X,E10.4)
1045 FORMAT(1HO,7X,31HEFFECTIVE CONDITIONS(CGS UNITS),//,
     +    2X,5HPEFFC,15X,E10.4/
     +    2X,5HVEFFC,15X,E10.4/
     +    2X,6HROEFFC,14X,E10.4/
     +    2X,5HAEFFC,15X,E10.4/
     +    2X,6HRAEFFC,14X,E10.4/
     +    2X,5HHEFFC,15X,E10.4/
     +    2X,5HTEFFK,15X,E10.4)
1055 FORMAT(1HO,//2X,10HTUOXOK (K),6X,E10.4/
     +              2X,10HDTDXMK (K),6X,E10.4/
     +              2X,10HDTDUMK (K),6X,E10.4/
     +              2X,10HTUOXXK (K),6X,E10.4/
     +              2X,8HTCPK (K),8X,E10.4)
1056 FORMAT(1HO,//2X,13HHNOT (CAL/GM),3X,E10.4/
     +              2X,14HDHDXM (CAL/GM),2X,E10.4/
     +              2X,13HHXOM (CAL/GM),3X,E10.4/
     +              2X,12HHCP (CAL/GM),4X,E10.4/
     +              2X,13HHCPC (ERG/GM),3X,E10.4)
1057 FORMAT(1HO,//2X,13HROCPC (GM/CC),3X,E10.4/
     +              2X,10HGAMCPC (-),6X,E10.4/
     +              2X,13HUCPC (CM/SEC),3X,E10.4/
     +              2X,14HAOCPC (CM/SEC),  2X,E10.4/
     +              2X,16HCPCPC (ERG/GM K),1X,E10.4)
1022 FORMAT(1HO,2X,33HDISTANCE FROM PLATE TO PROBE (CM),2X,E10.4/
     +              2X,31HVEL AT PROBE WITH PLATE(CM/SEC),4X,E10.4)
1060 FORMAT(1HO,//2X,2HAC,18X,E10.4/
     +      2X,5HKAPPA,15X,E10.4/
     +      2X,5HDENOM,15X,E10.4)
1065 FORMAT(1HO,//2X,6HROAIRC,14X,E10.4/
     +      2X,4HACPC,16X,E10.4/
     +      2X,5HRACPC,15X,10.4)
1067 FORMAT(1H ,//2X,3HVAC,17X,E10.4/
     +              2X,5HRADAC,15X,E10.4/
     +              2X,6HHEQCPC,14X,E10.4/
     +              2X,3HHAC,17X,E10.4/
     +              2X,3HTAK,17X,E10.4)
2000 CALL EXIT
```

DISTRIBUTION LIST

No. of Copies	Organization
12	Administrator Defense Documentation Center ATTN: DTIC-DDA Cameron Station Alexandria, VA 22314
1	Commander US Army Materiel Development & Readiness Command ATTN: DRCMD-ST 5001 Eisenhower Avenue Alexandria,VA 22333
2	Commander US Army Armament Research & Development Command ATTN: DRDAR-TSS Dover, NJ 07801
1	Commander US Army Armament Material Readiness Command ATTN: DRSAR LEP-L,Tech Lib. Rock Island,IL 61299
1	Commander US Army Aviation Research & Development Command ATTN: DRDAV-E 4300 Goodfellow Blvd. St.Louis, MO 63120
1	Director US Army Air Mobility Research & Development Laboratory Ames Research Center Moffett Field, CA 94035
1	Commander US Army ARRADCOM Benet Weapons Laboratory ATTN: DRDAR-LCB-TL Watervliet,NY 12189
1	Commander US Army Armament Research & Development Command ATTN: DRDAR-TDC Dover, NJ 07801
1	Commander US Army Communications Rsch & Development Command ATTN: DRDCO-PPA-SA Fort Monmouth, NJ 07703
1	Commander US Army Electronics Research & Development Command Technical Support Activity ATTN: DELSD-L Fort Monmouth, NJ 07703
2	Commander US Army Missile Command ATTN: DRSMI-R DRSMI-YDL Redstone Arsenal, AL 35898
1	Commander US Army Tank Automotive Research & Development Cmd ATTN: DRDTA-UL Warren, MI 48090
1	Director US Army TRADOC Systems Analysis Activity ATTN: ATAA-SL, Tech Lib White Sands Missile Range NM 88002
50	Department of Transportation Federal Railroad Administration Office of Rail Safety Research ATTN: Mr.D.Levine, Program Manager, FRA/RRD-33 7th and D Sts., SW Washington,D.C. 20590
5	National Railroad Passenger Corp. ATTN: E.J.Lombardi,Eng.of Tests 400 N.Capitol St.,N.W. Washington,D.C.20001
1	Southwest Research Institute 6620 Culebra Road San Antonio, TX 78284

DISTRIBUTION LIST

Aberdeen Proving Ground

Director, USAMSAA
ATTN: DRXSY-D
DRXSY-MP, H. Cohen
B. Cummings

Commander, USATECOM
ATTN: DRSTE-TO-F

Director, USACSL
Bldg. E3516 EA
ATTN: DRDAR-CLB-PA

USER EVALUATION OF REPORT

Please take a few minutes to answer the questions below; tear out this sheet, fold as indicated, staple or tape closed, and place in the mail. Your comments will provide us with information for improving future reports.

1. BRL Report Number _____

2. Does this report satisfy a need? (Comment on purpose, related project, or other area of interest for which report will be used.)

_____

_____

_____

3. How, specifically, is the report being used? (Information source, design data or procedure, management procedure, source of ideas, etc.) _____

_____

_____

4. Has the information in this report led to any quantitative savings as far as man-hours/contract dollars saved, operating costs avoided, efficiencies achieved, etc.? If so, please elaborate.

_____

_____

5. General Comments (Indicate what you think should be changed to make this report and future reports of this type more responsive to your needs, more usable, improve readability, etc.) _____

_____

_____

_____

6. If you would like to be contacted by the personnel who prepared this report to raise specific questions or discuss the topic, please fill in the following information.

Name: _____

Telephone Number: _____

Organization Address: _____

_____

_____

FOLD HERE

Director
US Army Ballistic Research Laboratory
Aberdeen Proving Ground, MD 21005

NO POSTAGE
NECESSARY
IF MAILED
IN THE
UNITED STATES

OFFICIAL BUSINESS
PENALTY FOR PRIVATE USE, $300

BUSINESS REPLY MAIL
FIRST CLASS PERMIT NO 12062 WASHINGTON, DC
POSTAGE WILL BE PAID BY DEPARTMENT OF THE ARMY

Director
US Army Ballistic Research Laboratory
ATTN: DRDAR-TSB-S
Aberdeen Proving Ground, MD 21005

FOLD HERE


FILMED
9 8